Type of article: Original Article

Functional analysis of the taproot and fibrous roots of *Medicago truncatula:* sucrose and proline catabolism primary response to water deficit.

Veronica Castañeda[a], Marlon de la Peña[b], Lidia Azcárate[a], Iker Aranjuelo[c] and Esther M. Gonzalez[a*]

Addresses:

[a] Department of Environmental Sciences, Public University of Navarra, E-31006 Pamplona, Spain.

[b] Department of Plant Biology and Ecology, University of the Basque Country E-48080 Bilbao, Spain

[c] Institute of Agrobiotechnology, IdAB-CSIC-UPNA-Government of Navarre, E-31192 Mutilva, Navarre, Spain

***Corresponding author:** Esther M. Gonzalez, Department of Environmental Sciences, Public University of Navarra, Campus Arrosadia, 31006-Pamplona, Spain. Phone number: + 34 948 168412, email: esther.gonzalez@unavarra.es

Running title: Taproot and fibrous root response to water deficit stress

Submission date: July 2017

Number of tables: 0

Number of figures: 8 (Fig 1 and 4: color online)

Total Word count: 10.044 (including references)

Supplementary Data: 3 figures, 2 table

Abstract

Root performance represents a target factor conditioning plant development under drought conditions. Moreover, recent root phenotyping studies remark relevant differences on functionality of the different root types. However, despite its relevance, the performance of different types of roots such as primary/taproot (tapR) and lateral/fibrous roots (fibR) under water stress conditions is largely unknown. In the current study, the impact of water stress on target C and N metabolism (namely sucrose and proline) processes were characterized in tapR and fibR of *Medicago truncatula plants* exposed to different water stress severity regimes (moderate *versus* severe). While both root types exhibit some common responses to face water stress, the study highlighted important physiological and metabolic differences between them. The tapR proved to have an essential role on carbon and nitrogen partitioning rather than just on storage. Moreover, this root type showed a higher resilience towards water deficit stress. Sucrose metabolization at sucrose synthase level was early blocked in this tissue together with a selective accumulation of some amino acids such as proline and branched chain amino acids, which may act as alternative carbon sources under water deficit stress conditions. The decline in respiration, despite the over-accumulation of carbon compounds, suggests a modulation at sucrose cleavage level by sucrose synthase and invertase. These data not only provide new information on the carbon and nitrogen metabolism modulation upon water deficit stress but also on the different role, physiology, and metabolism of the taproot and fibrous roots. In addition, obtained results highlight the fact that both root types show distinct performance under water deficit stress; this factor can be of great relevance to improve breeding programs for increasing root efficiency under adverse conditions.

Keywords: Amino acids, carbon metabolism, invertase, lateral roots, nitrogen metabolism, sucrose synthase.

Abreviations: *AAT*, aspartate aminotransferase; *ADH*, alcohol dehydrogenase; *AGPase*, ADP-glucose pyrophosphorylase; *AlaAT*, alanine aminotransferase; *AP*, alternative pathway; *BCAA*, branched chain amino acids ; *C*, control; *CE*, capillary electrophoresis; *CP*, cytochrome pathway; DW, dry weight; *FBPase*, fructose 1,6-bisphosphatase; *fibR*, fibrous root; *FW*, fresh weight; *G6PDH*, glucose-6-phosphate dehydrogenase; *GDH*, glutamate dehydrogenase; *GOGAT*, glutamine oxoglutarate aminotransferase/glutamate synthase; *GAPDH*, glyceraldehyde-3-phosphate dehydrogenase; *GPDH*, glycerol-3-phosphate dehydrogenase; *HK*, hexokinase; *IDH*, isocitrate dehydrogenase; *INV*, invertase; *MD*, moderatewater deficit; *MDH*, malate dehydrogenase; *ME*, NADP-malic enzyme; *OPP*, oxidative pentose phosphate pathway; *ProDH*, proline dehydrogenase; *P5CS*, pyrroline-5-carboxylate synthase; *PDC*, pyruvate decarboxylase; *PK*, pyruvate kinase; *rR*, residual respiration; SD, severewater deficit; *SKDH*, shikimate dehydrogenase; *SuSy*, sucrose synthase; *T*, transpiration; *tapR*, taproot; *tR*, total respiration; *UGPase*, UDP-glucose pyrophosphorylase; *WC*, water content.

1. Introduction

Legumes are characterized by their high nutritional value for humans and livestock and by their ecological value as nitrate suppliers through their symbiosis with nitrogen-fixing bacteria (Graham and Vance, 2003). These advantages are however compromised by their low ability to adapt to adverse environmental conditions such as drought (Zahran, 1999). Within a climate change context, it is of great importance to maintain/increase their yield in stressful growth conditions to meet the economical requirements of the increasing world population. In order to achieve this, it is mandatory to further understand the adaptive response of these plants to water-deficit stress and select particular traits that allow them to better cope with the lack of water in the soil. *Medicago truncatula* is a model legume cultivated as an annual forage in several regions worldwide (Michaud *et al.*, 1988) and phylogenetically related to some of the most relevant European legume crops (Aubert *et al.*, 2006; Phan *et al.*, 2007). While grain legumes are generally described as drought sensitive (González et al., 1995, 1998, Ramos et al., 1994), forage legumes as *M. truncatula* has been described to exhibit a higher tolerance to dry enviroments (Araújo *et al.,* 2015).

Roots are essential for plant productivity and serve a variety of functions, such as anchorage and water and nutrient absorption. Tap or primary roots are those formed in the embryo growing directly downwards whilst lateral roots are those formed post-embryonically emerging from the pericycle, being root architecture determined by genetic, physiological, and environmental factors (Lynch and Brown, 2012). In general, cultivated legumes develop a tap root system with a strongly developed primary root with branches. In the perennial alfalfa, the taproot has been described as the main underground storage organ, acting as a carbon and nitrogen reservoir to drive the regrowth after cutting (Erice et al., 2011). Despite being a close relative of alfalfa, the root system of the model legume *M. truncatula* consists of numerous

86 branches emerging from a short taproot located at the upper side, appearing similar to the
87 fibrous root system of monocots.

88 Plant roots are starting to gain interest regarding their role in drought stress tolerance
89 (Sutka et al., 2016; Zhan et al., 2015). Indeed, the identification of root mechanisms improving
90 drought tolerance it is essential to design drought tolerant crops (Lynch et al., 2014). Despite
91 the importance of the root system as the first organ encountering soil water deficit, its response
92 to drought stress has not been as extensively studied as the green parts. Besides, the vast
93 majority of studies focused on the root system regard it as a whole without distinguishing root
94 types that emerge from it despite their particular anatomical and physiological characteristics
95 (Tian et al., 2014). Gewin (2010) points to the role of plant roots to improve plant stress
96 tolerance, attending among others to factors related to anatomical-morphological characteristics
97 of the different root types. Studies conducted during the last decade show a clear interaction
98 between environmental conditions (such as drought) and legume taproot development by
99 trapping the vegetative storage proteins and avoiding their export towards the shoot for
100 regrowth production (Erice et al., 2007). Physiological differences between taproot and lateral
101 roots have also been suggested in *Faba bean* related to lipid metabolism (Waisel and Radunz,
102 2006). In addition, an increased taproot diameter has been identified as key component in
103 providing a deeper root system in white clover under drought-prone environments (Woodfield
104 et al., 1996). In *M. truncatula*, scarce information is available, being root morphology a
105 neglected issue (Moreau, 2006). However, the relevance of different root properties has been
106 demonstrated comparing the response of tolerant and sensitive cultivars to drought stress, with
107 roots developing not only structural changes but also physiological, such as an increase of
108 osmoregulating properties of the root cells in durum wheat (Bajji et al., 2000), an improved
109 efficiency of water absorption in tall fescue (Huang and Gao, 2000), or the synthesis of
110 protective molecules in *Brassica juncea* (Phutela et al., 2000).

Osmotic adjustment has been proved as a prime adaptive trait in support of crop yield under drought conditions (Blum, 2017). Amino acids are key players in this osmotic adjustment, highlighting proline by its role in cellular homeostasis, including redox balance and energy status (Szabados and Savouré, 2010). It has been shown that proline pools supply a reducing potential for mitochondria through the oxidation of proline, providing electrons for the respiratory chain and therefore contribute to energy supply for resumed growth (Kishor et al., 2005). In addition, carbohydrates often accumulate in the form of abundant sugars such as hexoses and sucrose, dismissing the prediction of a carbon starvation provoked by a reduced photosynthetic rates under water deficit (Muller et al., 2011). Although in this context an osmoprotective role has been associated to carbohydrates (Gil et al., 2013), growth and development of sink organs is known to be, at least partly, under the control of C availability (Muller et al., 2011).

In the current study, we characterize the physiology and metabolism of the taproot and fibrous root of *M. truncatula* plants under control and moderate and severe water deficit conditions. Special attention has been paid to the metabolism of sucrose and proline, which has been shown to be modulated in both root types and stress conditions. Results revealed physiological and metabolic differences between both root types under control condition and distinct performance under water deficit stress suggesting different roles in the physiology of the whole plant root system.

2. Materials and methods

2.1. Plant material, growth conditions and experimental design

M. truncatula seeds were scarified with sulfuric acid 98% for 7 min, washed and then sterilized with 3.5 % sodium hypochlorite for 90 seconds. After a thorough wash, the seeds were soaked

in water and left shaking in the dark for 6 hours. When the seeds were hydrated, they were transferred to 7‰ agar plates at 4 ºC for one day in the dark, and then incubated at 20 ºC for two days. The seedlings were then planted in pots with perlite:vermiculite (1:3, v/v) and grown under controlled conditions (22/18 ºC day/night temperature, 70% relative humidity, 500 µmol m^{-2} s^{-1} (PPF), 12 h photoperiod) and irrigated with Evans medium supplemented with 5 mM NH_4NO_3 (Evans, 1981).

Six-week-old plants were randomly separated into three sets containing ten biological replicates each. Water deficit stress was then imposed by water withdrawal and the hydric status of the water-deprived and control (well-watered) plants was monitored daily by measuring the water potential of the leaves. During the water deficit study, control (C) plants were irrigated with water to avoid nutritional differences. When the leaf water potential (Ψ_w) of the water deficit stressed plants reached the desired value (for moderate deficit (MD) Ψ_w= -1.51 ± 0.02 MPa, 6-7 days treatment and for severe deficit (SD) Ψ_w= -2.5 ± 0.04 MPa, 8-9 days treatment), plants were harvested by separating the primary root (tapR) from the lateral fibrous roots (fibR) with a scalpel and flash-freezing both in liquid nitrogen, except for the samples used in respiration measurements, which were measured *in situ*. Control plants were harvested all along the 9 total days of harvesting, showing an average Ψ_w of -0.37 ± 0.01 MPa. Samples were stored at -80 ºC for further analysis. The number of biological replicates employed for the different analyses are indicated in the respective figure legends.

2.2. Plant water status

Plant transpiration (T) was gravimetrically determined on a daily basis. Ψ_w was measured in the second fully expanded leaf 2 h after the beginning of the photoperiod using a pressure chamber (Soil Moisture Equipment, Santa Barbara, CA, USA) as earlier described (Scholander et al., 1965). Water content was determined in the base to the fresh weight (FW) and the dry

159 weight (DW) obtained after 48 hours drying at 70 ºC using the following formula: WC (%) =
160 (FW-DW) *100/FW.

161 *2.3. Respiration measurements*

162 Root respiration (O_2 consumption at 21 °C) was measured using a Clark-type O_2 electrode
163 (Hansatech Oxygraph, H. Sabur Laborbedarf, Reutlingen) connected to constant temperature
164 circulating water baths at 25 ºC. For each plant, two root aliquots (0.05 g FW) were placed into
165 two tightly closed oxygraph chambers containing 1 ml reaction buffer (25 mM imidazole-HCl,
166 pH 6.5) under stirring. After a constant rate of oxygen uptake was attained, 10 µl of 0.01 M
167 KCN in 20 mM HEPES, pH 8 or 20 µl of 1 M SHAM in 2-methoxyethanol were added to each
168 chamber, respectively. About 5 min after the application of the first inhibitor, the other inhibitor
169 was added. Total Respiration (tR) was determined as the rate of O_2 consumption before the
170 addition of any inhibitor, while the residual respiration (rR) was determined as the O_2
171 consumption in the presence of both SHAM and KCN. The alternative pathway (AP) capacity
172 was calculated by substracting the rR from the O_2 consumption rate obtained after inhibiting
173 the cytochromic pathway with KCN, while the cytochrome pathway (CP) capacity was
174 calculated in a similar way but after inhibiting the alternative pathway with SHAM.

175 *2.4. Determination of free amino acid content*

176 Frozen samples were ground to powder under liquid N_2 and subsequently homogenized using
177 a mortar and pestle with 1 M HCl (≈10 ml g FW^{-1}) and incubated on ice for 10 min.
178 Subsequently, extracts were centrifuged at 20,000 *g* and 4 ºC for 10 min. Supernatants were
179 neutralized using NaOH, and internal standards norvaline and homoglutamic acid were spiked.
180 Then, samples were derivatized with 1 mM FITC dissolved in acetone at room temperature for
181 15 h in 20 mM borate buffer (pH 10). The content of free amino acids was determined using a
182 Beckman Coulter capillary electrophoresis (CE) PA-800 (Beckman Coulter Inc., USA) coupled

to laser-induced fluorescence detection (argon laser at 488 nm), as described in (Arlt et al., 2001; Takizawa and Nakamura, 1998), with minor modifications. A fused-silica capillary, 43/53.2 cm long and 50 μm internal diameter (Beckman Coulter Inc., USA), was employed. For amino acid separation, 45 mM α-cyclodextrin in 80 mM borax buffer (pH 9.2) was used. Analyses were performed at 20 ºC and at a voltage of 30 kV (110 uA). Total amino acid content on a DW base is presented as the summation of single amino acids for each sample.

2.5. Determination of soluble sugars and starch content

Soluble sugars were extracted as detailed in Gálvez et al. (2005). Frozen material was exhaustively extracted three times in boiling ethanol (80% v/v) for 30 seconds and once more time at RT. The aqueous phase of the ethanol extract was evaporated at 40 ºC using a Turbovap LV evaporator (Zymark Corp. Hopkinton, MA, USA) for soluble sugar determination. After the evaporation cycle, the dry residue was resuspended in dH_2O by vigorous vortexing. A sample cleaning was then performed by centrifugation for 10 minutes and the supernatants were stored at -20 ºC for further analysis.

The remaining tissue after ethanol soluble compound extraction was dried at 70ºC for 48 hours. Dry samples were homogenized with water using mortar and pestle and further boiled for one hour for starch grain breakage. After cooling down, 1 ml of desalted amyloglucosidase solution (EC 3.2.1.3, 0.5 units/ml acetate buffer pH 4.5) was added to each tube and incubated under shaking at 55 ºC for starch digestion. Extractions were centrifuged at 2330 *g* for 10 minutes and the supernatants were stored at -20 ºC for further glucose quantification. Sucrose, glucose, and fructose were determined by CE in a Coulter PACE system 5500 (Beckman) coupled to a diode array detector (Marino et al., 2006). Concentrations were calculated from peak heights using commercial standards (Sigma–Aldrich, Germany). The total amino acid content was calculated as the sum of the 20 standard amino acids synthesized in plants and the non-proteogenic γ-aminobutyric acid (GABA).

208 *2.6. Determination of total soluble protein content and enzymatic activities*

209 Aliquots of frozen roots (≈1 g) were ground into a fine powder with liquid nitrogen and
210 homogenized with extraction buffer (50 mM MOPS pH 7.5, 0.1% (v/v) Triton X-100, 10 mM
211 $MgCl_2$, 1 mM EDTA, 20 mM KCl, 10 mM DTT, 10 mM β-mercaptoethanol, 2.5% PVPP, 2
212 mM PMSF and a protease inhibition cocktail tablet) and centrifuged at 24000 *g* and 4 ºC for 20
213 minutes. The protein content of the supernatant was determined by the Bradford assay in the
214 crude extract using BSA as protein standard.

215 Additionally, the crude protein extract was also employed to determine the activity of
216 glutamate synthase (GOGAT, EC 1.4.1.14), proline dehydrogenase (ProDH, EC 1.5.5.2),
217 pyrroline-5-carboxylate synthase (P5CS, EC not assigned), ADP-glucose pyrophosphorylase
218 (AGPase, EC 2.7.7.27) and pyruvate decarboxylase (PDC, EC 4.1.1.1). An aliquot of this
219 extract was desalted through BioGel P-6 DG Desalting Gel (BioRad) equilibrated with desalting
220 buffer (250 mM MOPS pH 7.5, 50 mM $MgCl_2$, 100 mM KCl) to determine the activity of
221 alcohol dehydrogenase (ADH, EC 1.1.1.1), UDP-and ADP-sucrose synthase (SuSy, EC
222 2.4.1.13), UDP-glucose pyrophosphorylase (UGPase, EC 2.7.7.9), malate dehydrogenase
223 (MDH, EC 1.1.1.37), acid and alkaline invertases (INV, EC 3.2.1.26), aspartate
224 aminotransferase (AAT, EC 2.6.1.1), alanine aminotransferase (AlaAT, EC 2.6.1.2), shikimate
225 dehydrogenase (SKDH, EC 1.1.1.25), glucose-6-phosphate dehydrogenase (G6PDH, EC
226 1.1.1.49), glutamate dehydrogenase (GDH, EC 1.4.1.2), fructose-1,6-bisphosphatase (FBP, EC
227 3.1.3.11), glyceraldehyde-3-phosphate dehydrogenase (GAPDH, EC 1.2.1.11), NADP-
228 isocitrate dehydrogenase (IDH, EC 1.1.1.41), NADP-malic enzyme (ME, EC 1.1.1.40),
229 glycerol-3-phosphate dehydrogenase (GPDH, EC 1.1.5.3), pyruvate kinase (PK, EC 2.7.1.40)
230 and hexokinase (HK, EC 2.7.1.1). Enzymatic activities were assayed spectrophotometrically as
231 the oxidation or reduction of NAD(P)(H) nucleotides at 30 ºC and 340 nm for 15 min after an
232 initial incubation of 5 min at RT before the substrate addition.

PDC, ADH, SuSy, acid and alkaline INV, UGPase, MDH and GOGAT were assayed as Gonzalez et al. (1998), AAT and AlaAT as Hatch and Mau (1973), ProDH and P5CS as Rouached et al. (2013), SKDH, G6PDH, GDH, FBPase, GAPDH and IDH as Gibon et al. (2004), ME as Ryšlavá et al. (2003), GPDH as Shen et al. (2006), AGPase as Baroja-Fernandez et al. (Baroja-Fernández et al., 2003), PK as Wood (1968) and HK as Sigma protocols, with minor modifications. Enzymatic activities were expressed on a protein basis in order to visualize possible regulation mechanisms in response to water deficit stress.

2.7. Statistical analysis

Multiple comparison analyses were performed with SPSS using analysis of variance (ANOVA, $P \leq 0.05$) and Duncan´s test. Student´s t-test ($p \leq 0.05$) was performed when a single comparison was needed.All data are reported as the mean ± standard error of n = 5-10 independent measurements. The number of biological replicates employed for the different analyses are indicated in the respective figure legends.

3. Results

Control plants exhibited a leaf Ψ_w value of -0.37 ± 0.01 MPa. Plants entered a moderate level of water deficit stress (MD) 6-7 days after water deficit stress imposition and were harvested when their leaf Ψ_w reached -1.51 ± 0.02 MPa. On the other hand, the severe stressed plants (SD) were harvested after 8-9 days treatment with an average Ψ_w of -2.51 ± 0.04 MPa. Significant differences of shoot and root DW biomass were not observed due to the short-time study period employed although a slight upward trend of the shoot to root ratio is inferred **(Fig. S1A, Table S2)**. A visual loss of turgor correlated with the general decline in the water content (WC) and significant differences were observed between the response of the different organs (**Fig. 1, Table S2**). Water content of leaves and tapR decreased around 15% under SD, while fibR WC decreased 30 and 65% under MD and SD, respectively. Transpiration gradually

257 decreased from two days after the beginning of the water deficit treatment, whilst leaf Ψ_w did
258 not significantly decrease until the fifth day of water deficit stress, exhibiting afterward a
259 continuous drop (**Fig. S1B, C**).

260 Water deficit stress led to a decline in the total root respiration of both tapR and fibR,
261 with the response of the latter being more abrupt than that of the tapR (**Fig. 2A**). In the tapR,
262 the total respiration rate declined 2-fold in SD compared to C, while the respiration drop for the
263 fibR was 4-fold. Residual respiration (rR), measured after inhibiting alternative and cytochrome
264 pathways, was similar in both root types under control conditions (**Fig. 2B**), accounting for the
265 29% and 23% of the total measured respiration for the tapR and fibR, respectively. The
266 moderate water deficit stress imposition led to an increase in the rR of the tapR, followed by a
267 decline under severe conditions. In the case of the fibrous root, rR decreased abruptly to half
268 the value under moderate conditions, remaining low under severe conditions. However, when
269 rR values were relativized for the total root respiration, a statistically significant increase was
270 observed for both root types under water deficitstress conditions, suggesting an activation of
271 oxidative processes becoming more pronounced in the tapR (**Fig. 2B**). Overall, ANOVA
272 analysis showed a significant interaction between water deficit treatment and organ which
273 support the different water deficit response observed in both root types **(Table S2).**

274 Under control conditions, as it has been observed for the total respiration rate, the
275 alternative (AP) and cytochrome pathway (CP) capacities were higher in the fibR than the tapR
276 (**Fig. 2 C, D, Table S1**). Both respiration capacities declined in response to water deficit stress,
277 being CP the most affected one with a 4- and 15-fold decrease in the tapR and fibR, respectively.
278 AP capacity declined significantly in the fibR under both stress conditions, but in the taproot
279 this effect was only significant under severe water deficit. In addition, not only the decline in
280 both capacities was different for each root type, but also the AP:CP ratio differed from one root
281 type to the other. In both cases, despite the decrease in the measured AP and CP capacities,

water deficit stress led to a similar increase in the relative AP capacity in detriment of the CP, with these changes being already statistically significant under MD in the case of the fibR (**Fig. 2 C, D**).

Water deficit stress provoked a reduction of the soluble protein content in both root tissues, being the effect more pronounced in the fibR (**Fig. 3A**). Under control conditions, the amino acid content was higher in the tapR than in the fibR (**Fig. 3B**), as it can also be observed for many of the single amino acids (**Fig. S2**)**.** Under control conditions there is a clear supremacy of Asn in the fibrous root (74%) contrasting with a more diverse composition of the taproot, which held significant amounts of Asn (47%), GABA (11%), Ser (11%) and Pro (6%) (**Fig. 4A**). The amino acid levels increased in response to water deficit stress in both root tissues (**Fig. 3B**). **Figure 4B** represents the relative log fold change of each amino acid in the tapR and fibR in response to MD and SD. In the fibR, the only significant changes (≥ 2) in response to water deficit stress were the accumulation of Pro, His, and Trp together with a decrease in Gly content. Conversely, in the tapR water deficit stress provoked a more marked effect at amino acid level. Thus, in addition to Pro and His, a significant increase of the branched chain amino acids and a decrease of Gln, GABA, Glu and Asp were observed in the tapR (**Fig. 4B**). However, the Asn pool was quite steady in both root types under water deficit conditions (**Fig. 4B**). ANOVA analysis showed a significant interaction for the total amino acid content and most of the amino acids, supporting the differential response exhibited by the nitrogen compounds depending on the root type **(Table S2, Fig. S2)**.

Under control conditions, sucrose were more abundant in tapR than in the fibR (**Fig. 5A**) whilst starch did not reach to show significant differences **(Fig. 5B)**. Conversely, regarding hexoses, glucose was significantly more abundant in the fibR whilst fructose did not reach to increase significantly (**Fig. 5C, D**). Upon water deficit stress, sucrose content increased 3- and 8- fold in the tapR and fibR, respectively **(Fig. 5A)**, while the hexoses, glucose and fructose,

accumulated exclusively in the fibR **(Fig. 5)**. Thereby, ANOVA analysis reported a significant interaction for both hexoses **(Table S2)**.

Among the measured enzymatic activities, only those whose activity was significantly affected by water deficit stress are shown in **Figures 6 and 7**, while those enzymatic activities showing non-significant differences are represented in **Fig. S3**. Related to root nitrogen assimilation, GOGAT was up-regulated in the fibR at the time that AAT and AlaAT were down-regulated (**Fig. 6A-C**). Conversely, these primary nitrogen assimilation enzymes remained unaffected in the tapR. P5CS and ProDH catalyze the synthesis and degradation of proline, respectively. Water deficit stress did not affect P5CS in the tapR but led to a 2.4-fold increase in the case of the fibR (**Fig. 6D**). ANOVA analysis reported a significant interaction among water deficit treatment and organ for all the above mentioned nitrogen metabolism enzymes **(Table S2)**. However, ProDH activity was induced by water deficit in both root types, exhibiting a higher activity in the tapR than in the fibR (**Fig. 6E**). SKDH, involved in the biosynthesis of aromatic amino acids, decreased in both root types in response to water deficit stress (**Fig. 6F**). ANOVA analysis showed a significant effect in ProDH and SKDH enzymes for water deficit treatment and organ although a significant interaction between both factors was not observed since a similar increasing trend was observed in both root types **(Table S2)**.

Among the enzymes related to the carbon catabolism, both UDP- and ADP- SuSy decreased in response to water deficit (**Fig. 7 A, B**). In both root types, UDP-SuSy activity was as much as 40 times higher than that of the ADP-SuSy. UDP-SuSy activity decreased significantly in both root tissues even at moderate water deficit, and although a similar trend was observed, the response of ADP-SuSy was less pronounced than that of UDP-SuSy (**Fig. 7A, B**). Thereby, ANOVA analysis showed a significant interaction for ADP-Susy but this was not significant for UDP-Susy **(Table S2)**. Acid- and alkINV are also involved in the sucrose degradation route in the cell wall and cytosol, respectively, producing glucose and fructose in

an irreversible manner. AcidINV showed similar activities in both root types and declined significantly only under SD in the fibR (**Fig. 7C**). However, AlkINV was up to 4-fold more active than the AcidINV and it was significantly induced in the fibR even under moderate water deficit (**Fig. 7D**). ANOVA analysis showed a significant interaction for AlkINV but this was not significant for AcidINV **(Table S2)**. GPDH, a major link between the carbon and lipid metabolism, and G6PDH, a key enzyme of the pentose phosphate pathway, were both unaltered in the tapR when roots were subjected to water deficit stress (**Fig. 7 E, F**). However, they both exhibited a clear response in the fibR: GPDH activity increased 3 and 5.5-fold under MD and SD, respectively (**Fig. 7E**), while G6PDH showed a loss of activity concomitant with the water deficit stress level increment (**Fig. 7F**). ANOVA analysis showed a significant interaction among water deficit treatment and organ for GPDH and G6PDH enzymes **(Table S2)**.

Figure 8 represents the ratio tapR:fibR expressed in logarithmic basis for different enzyme activities, metabolites and physiological measurements under control conditions. Several enzymatic activities showed significant differences between both root types such as ADH and UGPase, which were 2-fold more active in the tapR than in the fibR (**Fig. 8A**). ProDH was also more active in the tapR than the fibR, even though a similar proline content was observed in both root types (**Fig. S2**). Conversely, GDH, AGPase, and AlkINV were around 7, 4 and 2.5-fold, more represented in the fibR than tapR, respectively (**Fig. 8A**). The tapR was enriched in sucrose and amino acids whilst glucose and fructose were more abundant in the fibR in agreement with a higher respiratory activity in this root type (**Fig. 8B, C**).

4. Discussion

4.1. Is the primary metabolism homogeneous in the whole root system?

In barrel medic, the primary root or tapR is restricted to the top of the root system, while the lateral or fibR emerging from it account (volume and weight-wise) for most of the root system (**Fig. 1**). This study addresses the differences between the tapR and fibR of *M. truncatula* to better describe their role at the whole plant level by examining the distribution of the different enzyme activities, metabolites and physiological measurements (**Fig. 1-7**) under control conditions. **Figure 8** summarizes all the measured parameters in this study as the tapR:fibR ratio on a logarithmic basis, allowing to show how the different parameters are represented in the different root types.

Attending to metabolic features, the tapR exhibited a remarkably high ADH activity which may be related to its thicker anatomy (**Fig. 8C**). ADH is related to the fermentative respiratory metabolism and maintenance of a constant NAD supply (Päpke et al., 2013) and increases under hypoxic conditions (Fox et al., 1994). Therefore, this double activity of ADH exhibited by the tapR suggests a role in carbon metabolism for this root type. Similarly, the high content of sucrose, the enhancement of UDP-SuSy and UGPase activities (**Fig. 8A**) and the limited accumulation of reserve compounds such as starch or proteins in the tapR in comparison to the fibR (**Fig. 8B**) reinforce its role on carbon partitioning rather than just on reserve storage. In addition, a role on starch storage is also dismissed attending to the activity of the enzyme AGPase, involved in the synthesis of ADP-glucose for the starch synthesis (Geigenberger, 2011), which is 5-times less active in the tapR than in the fibR. Similarly, ADP-SuSy which has also been related to ADP-glucose synthesis in the cytosol (Baroja-Fernández et al., 2003) is also less active in the tapR (**Fig. 8A**). The distribution of sucrose degrading enzymes between both root types is also remarkable; AlkINV is more abundant in the fibR than in tapR whereas UPD-SuSy behaves the opposite (**Fig. 8A**). Indeed, sucrose degraded via invertase requires two molecules of ATP to be converted into hexose-phosphates, while the SuSy pathway linked to UGPase requires only one molecule of PPi (Stitt, 1998), and therefore this different strategy

for sucrose metabolization in each root type could be related to the higher respiration rate exhibited by fibR compared to the tapR (**Fig. 2**). Even though the role of these sucrose degrading enzymes in plant metabolism is still a matter of debate (Vargas and Salerno, 2010), while SuSy has been traditionally assigned to the role of sucrose cleavage this role has also been assigned to INV in Arabidopsis roots (Lou et al., 2007). The high level of glucose and fructose in the fibR (**Fig. 8**) suggests a high rate of sucrose metabolization in the fibR, which is also in agreement with a higher activity of the pentose phosphate pathway as suggests the enhancement of G6PDH (**Fig. 7 and 8**). Regarding nitrogen metabolism, an important percentage of the soluble protein pool (around 40%) has been related to N storage in alfalfa taproots (Staswick, 1994). Conversely, in *M. truncatula*, the soluble protein content pool of tapR was similar to that of fibR, dismissing any N storage role based on proteins in this root type (**Fig. 8B**). However, an overall enrichment in free amino acids was observed in the tapR (**Fig. 8B).** This is the case for proline, postulated to function as nitrogen reservoir under stress (Albert et al., 2012). Accordingly, ProDH, a cytosolic enzyme activated by proline, exhibited a high activity in the tapR (**Fig. 8A**) suggesting that Pro catabolism may have a role on nitrogen partitioning. On the other hand, Asn, the most abundant amino acid and associated to N transport in the plant, exhibited a similar concentration in both root tissues (≈50 umols g DW^{-1}; **Fig. S2**). Nevertheless, when expressed in relative values, Asn accounted for the 74% of the bulk amino acid content of the fibR, which could be linked to the nutrient assimilation role of this root type (**Fig. 4**). This is supported by the high IDH and GDH activities detected in the fibR (**Fig. 8A**), enzymes mainly related to the supply of 2-oxoglutarate for ammonium assimilation (Fontaine et al., 2012; Hodges et al., 2003). ANOVA analysis exhibited a significant effect of the organ for many of the analysed parameters supporting important metabolic differences between both root types **(Table S2)**. In summary, specific features are present in each root type that suggest that they exert a different role in the physiology of the

405 whole plant root system. However, a storage role can be dismissed for the tapR, which seems
406 to have a particular metabolic endowment to deal with carbon and nitrogen partitioning.

407 *4.2. Common responses to water deficit stress in the whole root system*

408 Despite drought is one of the most important factors that inhibit photosynthesis, this decline
409 occurs late during the onset of water stress whilst other processes such as cell growth and
410 biosynthetic processes are rapidly affected at very moderate water potentials (Hsiao, 1973).
411 Gargallo-Garriga et al. (2014) showed that shoot and root exhibit an opposite metabolic
412 response to water deficit, playing the root a more active role in facing the effects of water deficit
413 stress. Through CO_2 assimilation, shoot provided carbohydrates (mainly in the form of sucrose)
414 to roots where they are mainly delivered to sustain root growth and respiration (Lambers et al.,
415 1996). Most of the studies on the response of the respiratory process to water deficit focused
416 on shoot (Flexas et al., 2006) being scarce the results available at root level. Respiration is the
417 main source of ATP needed for uptake, transport and assimilation of nutrients and provides root
418 cells with carbon skeletons for biosynthesis of cellular components. The present study shows
419 that a general and early decline of SuSy activity occurs in root tissue, supporting a role on
420 carbon supply for respiratory activity at this point (**Fig. 7A**). The sucrose derivative sugars,
421 glucose and fructose, accumulated in both root types although the differences were only
422 significant in the fibR (**Fig. 5C, D**), which could indicate that root respiration is not carbon
423 limited but down-regulated by other factors. Attending to primary metabolism, both SuSy and
424 INV can catalyse the cleavage reaction of sucrose. In Arabidopsis roots, cytosolic INV has been
425 shown to be essential for normal plant development, being able of compensating the loss of
426 SuSy activity but not vice-versa (Barratt et al., 2009). However, this compensation mechanism
427 did not work in other sinks as maize seeds (Cheng and Chourey, 1999). In the present study, the
428 compensatory role of AlkINV worked exclusively in the fibR (**Fig. 7**) which may suggest a
429 tissue-specific mechanism. Conversely, INV activity decreases in cereals when exposed to

430 water deficit (Barnabás et al., 2008). In the last decade, new roles are being explored in relation
431 with cell INV besides sucrose metabolization in primary metabolism (Ruan et al., 2010).

432 Regarding amino acids, the observed overall accumulation (**Fig. 3B**) is a common response
433 towards water deficit stress amongst various plant species and organs (Gil-Quintana et al., 2013;
434 Rouached et al., 2013). It is well known that protein biosynthesis is early hampered under
435 drought stress in harmony with plant cell growth (Hsiao, 1973). Overall the accumulation of
436 amino acids has been related to a reduced incorporation into new proteins rather than de novo
437 synthesis or increased proteolysis (Gil-Quintana et al., 2013). Our study showed how Pro and
438 His were the two amino acids that were accumulated in a larger extent in both root types; even
439 at moderate water deficit stress (**Fig. 4, S2**). Proline has been described to act as a compatible
440 compound for osmotic adjustment. More specifically, this amino acid has been described to
441 retain water and protect and stabilize macromolecules and structures from stress-induced
442 damage (Rouached et al., 2013). In plants, proline is synthesized mainly from glutamate, by the
443 P5CS enzyme whilst catabolism occurs via the sequential action of ProDH producing P5C from
444 proline, and P5C dehydrogenase which converts P5C to glutamate (reviewed in Szabados and
445 Savouré, 2010). Although P5CS activity was only induced in the fibR (**Fig 6D**), ProDH was
446 up-regulated in both tissues in response to water deficit stress (**Fig. 6E**). ProDH has been
447 described to be downregulated in other plants systems exposed to different water deficit stress
448 (Miller et al., 2005; Phutela et al., 2000; Rouached et al., 2013). Nevertheless, Verdoy et al
449 (2006) also observed a ProDH up-regulation in roots and nodules of salt-stressed *M. truncatula*
450 plants, suggesting that the induction exerted by the high proline concentration surpassed the
451 downregulation effect of dehydration under moderate stress conditions. The proline catabolism
452 can be used to generate energy and reducing equivalents for the TCA cycle (Kishor et al., 2005)
453 when the respiratory flux is blocked. On the other hand, the increase in the aromatic amino acid
454 pool in response to water deficit stress (**Fig 4B, S2**) despite this decrease in the shikimate

455 dehydrogenase activity (**Fig. 6**) may suggest an amino acid import from other organs of the
456 plant. In this context, Aranjuelo et al. (2011) showed a shoot to root transport of amino acids in
457 alfalfa plants exposed to water deficit stress.

458 Summarizing, both root types exhibited a similar strategy to face water deficit; respiration
459 decreased despite the over-accumulation of sucrose, whose cleavage was markedly
460 downregulated at SuSy level. Additionally, proline catabolism seems to be enhanced, which
461 could contribute to counterbalance the deficiencies in carbon metabolism throughout the
462 respiratory pathway.

463 *4.3. The taproot is more resilient to water deficit than the fibrous root: SuSy and ProDH are*
464 *first activated upon water deficit stress*

465 Despite the physiological and metabolic similarities under control conditions and the common
466 responses to water deficit observed in tapR and fibR discussed in sections 4.1 and 4.2, several
467 specific features in both root types are noticeablebeing supported by the numerous significant
468 interactions reported by the ANOVA analysis **(Table S2)**. The tapR was able to keep a higher
469 water content (> 65%) than the fibR, responding similarly to the aerial part (**Fig. 1**).
470 Accordingly, all measured parameters showed a better resilience towards water deficit stress in
471 the tapR. Total respiration rate decreased less markedly in the tapR than in the fibR, and the
472 alternative/cytochromic capacity ratio was not affected in the tapR under MD whilst it increased
473 almost 3-fold in the fibR at this water stress level (**Fig. 2 C, D**). Starch degradation was
474 unaffected in the tapR under MD whilst a 50% reduction was observed in the fibR (**Fig. 5B**).
475 In addition, most of the analysed enzymes were fully unaffected in the tapR, while responding
476 actively in the fibR (**Fig. 6, 7**).

477 However, despite the higher resilience exhibited by the tapR, some responses were readily
478 activated in this tissue, which may be interpreted as a primary response to water deficit at the

479 root level. The more marked effects observed in the tapR under MD affect UDP-Susy and
480 ProDH activities (**Fig. 6, 7**). UDP-SuSy was rapidly inhibited (**Fig. 7A**) in accordance with a
481 marked accumulation of sucrose (**Fig. 5**). This enzyme leads to the production of sugar
482 nucleotides, which can act as glucose donor in the synthesis of cellulose and callose (Winter
483 and Huber, 2000), although it is also a key enzyme in the metabolization of sucrose in sink
484 tissues (Zrenner et al., 1995). In nodules of grain legumes, the decline of SuSy at early stages
485 of water deficit has been suggested to be associated with the supply of malate to sustain nodule
486 respiration of infected cells (Gálvez et al., 2005; Gonzalez et al., 1998).

487 Similarly, ProDH activity exhibited also an early increase in tapR (**Fig. 6**) in accordance with
488 the rapid accumulation of proline in this root part (**Fig. S2**). ProDH transcript level response to
489 salt and water deficit is quite controversial and the up-regulation (Verdoy et al., 2006) and
490 down-regulation (Miller et al., 2005) have been documented in Medicago species. Recently, a
491 role in oxidizing excess proline and transferring electrons to the respiratory chain has been
492 indicated for ProDH in Arabidopsis (Cabassa-Hourton et al., 2016), which may act as an
493 alternative source of energy when carbon metabolism is being impaired (**Fig. 2, 7**). The slight
494 decrease of soluble protein in the tapR dismisses proteolysis to be the process responsible for
495 the sharp accumulation of amino acids in this part of the root, especially under MD (**Fig. 3**).
496 The BCAAs, Leu, Ile, and Val, had a higher absolute and relative presence under control
497 conditions and increased linearly upon water deficit stress in the tapR (**Fig. 4B, S2**).
498 Accordingly, Virlouvet et al. (2011) observed that BCAA biosynthesis was enhanced under
499 water-limited conditions and contributed to maintaining kernel yield in maize. Pires et al. (2016)
500 have recently shown in Arabidopsis plants that BCAA can be used as alternative electron donors
501 to the mitochondrial electron transport chain, reinforcing their role on water deficit tolerance
502 mechanism most likely delaying the onset of the stress. Therefore, in agreement with the higher
503 content of BCAA observed in the tapR when exposed to water deficit, respiration of this root

type exhibits a higher resilience to MD, not only at the total respiration rate but also attending to the AP/CP ratio (**Fig. 2**). In summary, the primary responses to water deficit observed at the tapR level under moderate water deficit point to a blockage of sucrose metabolization at UDP-SuSy level together with a selective accumulation of some amino acids such as Pro and BCCA, which may act as alternative carbon sources under water deficit stress conditions.

5. Conclusions

In conclusion, specific metabolic features are present in each root type that suggest that they exert a different role in the physiology of the whole plant root system**.** A storage role can be dismissed for the taproot, which seems to have a particular metabolic endowment to deal with carbon and nitrogen partitioning. Overall, both root types exhibited a similar strategy to face water deficit although the taproot exhibited a higher resilience. An early blockage of sucrose metabolism occurs at the level of sucrose synthase activity leading to a marked accumulation of sucrose in the root. The enhancement of proline catabolism in the root may contribute to counterbalance the deficiencies in carbon metabolism throughout the respiratory pathway. In addition, the differential resilience of taproot and fibrous root towards water deficit stress make it an interesting target of breeding programs improving plant tolerance towards stress focusing on the different functionally of the root system.

Acknowledgements

The authors would like to thank Gustavo Garijo for technical assistance.

Funding

527 VC was funded by the Basque Country Government (BFI-2012-97). This work was financed
528 by the Spanish Ministry of Economy and Competitiveness (AGL 2011-23738) and the Public
529 University of Navarra/Caja Navarra Foundation (7442-1941/2016).

530

531

532 **Legend to figures**

533 **Figure 1.** Water deficit stress applied to *M. truncatula* plants. *Above:* Visual appearance of
534 shoots and roots of 6-week old plants subjected to control (C) (Ψ_{leaf} = -0.37 ± 0.00 MPa),
535 moderate stress (MD) (Ψ_{leaf} = -1.51 ± 0.02 MPa) and severe stress (SD) (Ψ_{leaf} = -2.51 ± 0.03
536 MPa) conditions. *Below left:* water content (%) of the leaf, taproot and fibrous roots under C
537 (black), MD (white) and SD (grey) conditions. Bars represent the mean ± SE (n = 10). Different
538 letters indicate significant differences according to Duncan-test (P≤0.05). *Below right*: Detail
539 of taproot and fibrous root.

540 **Figure 2.** Total (A) and residual root respiration (B) of the taproot and fibrous root of *M.*
541 *truncatula* plants under C (black), MD (white) and SD (gray) conditions. In B, the values above
542 the bars represent the contribution of residual respiration (as %) to the total measured
543 respiration. Graphs C and D represent the changes in cytochrome (striped bars) and alternative
544 (dotted bars) respiration capacities of the taproot and fibrous roots, respectively. The values
545 above the bars represent the AP:CP ratios under the different water deficit regimes. Bars
546 represent the mean ± SE (n = 10). Different letters indicate significant differences according to
547 Duncan-test (P≤0.05).

548 **Figure 3.** Protein (A) and amino acid (B) content of the taproot and fibrous root of *M. truncatula*
549 under control (black), MD (white) and SD (gray) conditions. Bars represent the mean ± SE (n
550 = 10). Different letters indicate significant differences according to Duncan-test (P≤0.05).

551 **Figure 4.** Amino acid composition of *M. truncatula* taproot (TapR) and fibrous (FibR) root
552 under control conditions (A) and the relative fold change in response to moderate (MD) and
553 severe (SD) water deficit conditions (B). In figure A, those amino acids representing less than
554 3% of the total amino acid pool are pooled together in the pie chart tagged as "others". Asterisks
555 indicate significant differences between C and D treatments (Student′s t-test, $P \leq 0.05$).

556 **Figure 5.** Changes in sucrose (A), starch (B, measured as glucose released after starch
557 enzymatic breakdown), fructose (C) and glucose (D) contents (μmol g DW^{-1}) of *M. truncatula*
558 taproots and fibrous root under control (black), MD (white) and SD (gray) conditions. Bars
559 represent the mean ± SE (n = 6). Different letters indicate significant differences according to
560 Duncan-test ($P \leq 0.05$).

561 **Figure 6.** Enzymatic activities (nmol NADH min^{-1} μg $prot^{-1}$) related to the nitrogen metabolism
562 measured in the taproot and fibrous roots of *M. truncatula* under control (black), MD (white)
563 and SD (gray) conditions. Bars represent the mean ± SE (n = 5). Different letters indicate
564 significant differences according to Duncan-test ($P \leq 0.05$). *GOGAT*, glutamine oxoglutarate
565 aminotransferase/glutamate synthase; *AAT*, aspartate aminotransferase; *AlaAT*, alanine
566 aminotransferase; *P5CS*, pyrroline-5-carboxylate synthase; *ProDH*, proline dehydrogenase;
567 *SKDH*, shikimate dehydrogenase

568 **Figure 7**. Enzymatic activities (measured as nmol NADH min^{-1} μg $prot^{-1}$) related to the carbon
569 metabolism measured in the taproot and fibrous roots of *M. truncatula* under control (black),
570 MD (white) and SD (grey) conditions. Bars represent the mean ± SE (n = 5). Different letters
571 indicate significant differences according to Duncan-test ($P \leq 0.05$). *UDP-SuSy*, UDP-glucose
572 synthase; *ADP-SuSy*, ADP-glucose synthase; *AcidINV*, acid invertase; *AlkINV*, alkaline
573 invertase; *GPDH*, glycerol-3-phosphate dehydrogenase; *G6PDH*, glucose-6-phosphate
574 dehydrogenase

575 **Figure 8.** Distribution of enzymatic activities (A), metabolite contents (B) and respiration rates
576 (C) between both root types. Bars represent the log_2 of the ratio taproot: fibrous root for each
577 parameter under control conditions. Those parameters more abundant in the TapR (TapR:FibR
578 ratio higher than 1.5) are marked in black and those more abundant in the FibR (TapR:FibR ratio
579 lower than -1.5) are marked in white. The grey color is used for those parameters exhibiting
580 similar values in both root types. Asterisks indicate significant differences for a given parameter
581 between the values of the taproot and the fibrous root (Student′s t-test, $P \leq 0.05$). *AcidINV*, acid
582 invertase; *ADH*, alcohol dehydrogenase; *AGPase*, ADP-glucose pyrophosphorylase; *AlaAT*,
583 alanine aminotransferase; *AlkINV*, alkaline invertase; *AlternatP*, alternative pathway capacity;
584 *AAT*, aspartate aminotransferase; *CytocP*, cytochrome pathway capacity; *FBPase*, fructose 1,6-
585 bisphosphatase; *G6PDH*, glucose-6-phosphate dehydrogenase; *GDH*, glutamate
586 dehydrogenase; *GOGAT*, glutamine oxoglutarate aminotransferase/glutamate synthase;
587 *GAPDH*, glyceraldehyde-3-phosphate dehydrogenase; *GPDH*, glycerol-3-phosphate
588 dehydrogenase; *HK*, hexokinase; *IDH*, isocitrate dehydrogenase; *MDH*, malate dehydrogenase;
589 *ME*, malic enzyme; *ProDH*, proline dehydrogenase; *P5CS*, pyrroline-5-carboxylate synthase;
590 *PDC*, pyruvate decarboxylase; *PK*, pyruvate kinase; *ResidualR*, residual respiration; *SKDH*,
591 shikimate dehydrogenase; *SuSy*, sucrose synthase; *TotalR*, total root respiration; *UGPase*,
592 UDP-glucose pyrophosphorylase.
593
594 **Supplementary information.**
595 **Table S1.** Respiration rates (mmol O_2 s^{-1} g DW^{-1}) of the taproot and fibrous root total
596 respiration, residual respiration, alternative pathway and cytochrome pathway capacities under
597 C, MD and SD. Each value represents the mean ± SE (n = 10). Different letters indicate
598 significant differences according to Duncan-test ($P \leq 0.05$).

599 **Table S2.** Results of analyses of variance (ANOVA, P ≤0.05). Results of the two-way analyses
600 of variance (ANOVA) of the water content and the different respiration parameters (A), carbon
601 compounds (B), carbon metabolism-related enzymatic activitie (C), nitrogen compounds
602 (including the relative amino acid amount) (D) and nitrogen metabolism-related enzymatic
603 activities (E). Asterisk indicate significant differences: * indicates P-value under 0.05, **
604 indicates P-value under 0.01 and *** indicates P-value under 0.001. Factor 1 is water deficit
605 (WD) treatment (control, moderate and severe) and factor 2 is organ (tapR and fibR) and
606 WD*Organ indicate the interaction between both factors.
607 **Figure S1:** A: Plant biomass parameters (shoot DW, root DW and shoot to root ratio) of *M.*
608 *truncatula* plants under C (black), MD (white) and SD (gray) conditions. Different letters
609 indicate significant differences according to Duncan-test (P≤0.05). B: Leaf Ψ_w and C:
610 Transpiration rate of control (square) and water deficit-stressed plants (triangle) along the
611 experiment. Asterisks indicate significant differences between C and D treatments (Student′s t-
612 test, P ≤ 0.05). Each value represents the mean ± SE (n = 4-10).
613 **Figure S2.** Absolute amino acid content (µmol g DW^{-1}) in the taproot (dotted line) and fibrous
614 roots (continuous line) of *M. truncatula* under C, MD and SD conditions. Values are the mean
615 ± SE (n = 5). Different letters indicate significant differences according to Duncan-test
616 (P≤0.05).
617 **Figure S3.** Enzymatic activities (nmol NADH min^{-1} µg $prot^{-1}$) in the taproot (dotted line) and
618 fibrous root (continuous line) of *M. truncatula* under C, MD and SD conditions. Bars represent
619 the mean ± SE (n = 5). Different letters indicate significant differences according to Duncan-
620 test (P≤0.05). *UGPase*, UDP-glucose pyrophosphorylase; *AGPase*, ADP-glucose
621 pyrophosphorylase; *ME*, Malic enzyme; *MDH*, malate dehydrogenase; *FBPase*, fructose 1,6-
622 bisphosphatase; *HK*, hexokinase; *GAPDH*, glyceraldehyde-3-phosphate dehydrogenase; *GDH*,

623 glutamate dehydrogenase; *IDH*, isocitrate dehydrogenase; *PK*, pyruvate kinase; *ADH*, alcohol
624 dehydrogenase; *PDC*, pyruvate decarboxylase.
625
626

627 **References**

628 Albert, B., Le Cahérec, F., Niogret, M.F., Faes, P., Avice, J.C., Leport, L., Bouchereau, A.,
629 2012. Nitrogen availability impacts oilseed rape (Brassica napus L.) plant water status
630 and proline production efficiency under water-limited conditions. Planta 236, 659–676.
631 doi:10.1007/s00425-012-1636-8
632 Aranjuelo, I., Molero, G., Erice, G., Avice, J.C., Nogués, S., 2011. Plant physiology and
633 proteomics reveals the leaf response to drought in alfalfa (Medicago sativa L.). J. Exp.
634 Bot. 62, 111–23. doi:10.1093/jxb/erq249
635 Araújo, S.S., Beebe, S., Martin, C., Delbreil, B., González, E.M., Gruber, V., Lejeune-Henaut,
636 I., Link, W., Monteros, M.J., Prats, E., Rao, I., Vadez, V., Vaz Patto C., 2015. Abiotic
637 stress responses in legumes: strategies used to cope with environmental challenges. Crit.
638 Rev. Plant Sci. 34:1-3, 237-280, doi: 10.1080/07352689.2014.898450
639 Arlt, K., Brandt, S., Kehr, J., 2001. Amino acid analysis in five pooled single plant cell
640 samples using capillary electrophoresis coupled to laser-induced fluorescence detection.
641 J. Chromatogr. A 926, 319–325. doi:10.1016/S0021-9673(01)01052-4
642 Aubert, G., Morin, J., Jacquin, F., Loridon, K., Quillet, M.C., Petit, A., Rameau, C., Lejeune-
643 Hénaut, I., Huguet, T., Burstin, J., 2006. Functional mapping in pea, as an aid to the
644 candidate gene selection and for investigating synteny with the model legume *Medicago*
645 *truncatula.* Theor. Appl. Genet. 112, 1024–1041. doi: 10.1007/s00122-005-0205-y
646 Bajji, M., Lutts, S., Kinet, J., 2000. Physiological changes after exposure to and recovery
647 from polyethylene glycol-induced water deficit in roots and leaves of durum wheat

(Triticum durum Desf.) cultivars differing in drought resistance. J. Plant Physiol. 157, 100–108. doi:10.1016/S0176-1617(00)80142-X

Barnabás, B., Jäger, K., Fehér, A., 2008. The effect of drought and heat stress on reproductive processes in cereals. Plant Cell Environ. 31, 11–38. doi:10.1111/j.1365-3040.2007.01727.x

Baroja-Fernández, E., Muñoz, F.J., Saikusa, T., Rodríguez-López, M., Akazawa, T., Pozueta-Romero, J., 2003. Sucrose synthase catalyzes the de novo production of ADPglucose linked to starch biosynthesis in heterotrophic tissues of plants. Plant Cell Physiol. 44, 500–509. doi:10.1093/pcp/pcg062

Barratt, D.H.P., Derbyshire, P., Findlay, K., Pike, M., Wellner, N., Lunn, J., Feil, R., Simpson, C., Maule, A.J., Smith, A.M., 2009. Normal growth of Arabidopsis requires cytosolic invertase but not sucrose synthase. Proc. Natl. Acad. Sci. U. S. A. 106, 13124–13129. doi:10.1073/pnas.0900689106

Blum, A., 2017. Osmotic adjustment is a prime drought stress adaptive engine in support of plant production. Plant. Cell Environ. 40, 4–10. doi:10.1111/pce.12800

Cabassa-Hourton, C., Schertl, P., Bordenave-Jacquemin, M., Saadallah, K., Guivarc'h, A., Lebreton, S., Planchais, S., Klodmann, J., Eubel, H., Crilat, E., Lefebvre-De Vos, D., Ghelis, T., Richard, L., Abdelly, C., Carol, P., Braun, H.-P., Savoure, A., 2016. Proteomic and functional analysis of proline dehydrogenase 1 link proline catabolism to mitochondrial electron transport in Arabidopsis thaliana. Biochem. J. 473, 2623–2634. doi:10.1042/BCJ20160314

Cheng, W.-H., Chourey, P.S., 1999. Genetic evidence that invertase-mediated release of hexoses is critical for appropriate carbon partitioning and normal seed development in maize. TAG Theor. Appl. Genet. 98, 485–495. doi:10.1007/s001220051096

Erice, G., Irigoyen, J.J., Sánchez-Díaz, M., Avice, J.C., Ourry, A., 2007. Effect of drought,

673 elevated CO_2 and temperature on accumulation of N and vegetative storage proteins
674 (VSP) in taproot of nodulated alfalfa before and after cutting. Plant Sci. 172, 903–912.
675 doi:10.1016/j.plantsci.2006.12.013
676 Erice, G., Sanz-Sáez, A., Aranjuelo, I., Irigoyen, J.J., Aguirreolea, J., Avice, J.C., Sánchez-
677 Díaz, M., 2011. Photosynthesis, N2 fixation and taproot reserves during the cutting
678 regrowth cycle of alfalfa under elevated CO2 and temperature. J. Plant Physiol. 168,
679 2007–2014. doi:10.1016/j.jplph.2011.07.007
680 Evans, H.J., 1981. Symbiotic Nitrogen Fixation in Legume Nodules, in: T.C., M. (Ed.),
681 Research Experiences in Plant Physiology. Springer Berlin Heidelberg, New York, p.
682 294. doi:10.1007/978-3-642-96168-7_26
683 Flexas, J., Bota, J., Galmés, J., Medrano, H., Ribas-Carbó, M., 2006. Keeping a positive
684 carbon balance under adverse conditions: responses of photosynthesis and respiration to
685 water stress. Physiol. Plant. 127, 343–352. doi:10.1111/j.1399-3054.2006.00621.x
686 Fontaine, J.X., Tercé-Laforgue, T., Armengaud, P., Clément, G., Renou, J.P., Pelletier, S.,
687 Catterou, M., Azzopardi, M., Gibon, Y., Lea, P.J., Hirel, B., Dubois, F., 2012.
688 Characterization of a NADH-dependent glutamate dehydrogenase mutant of Arabidopsis
689 demonstrates the key role of this enzyme in root carbon and nitrogen metabolism. Plant
690 Cell 24, 4044–4065. doi:10.1105/tpc.112.103689
691 Fox, T.C., Kennedy, R.A., Rumpho, M.E., 1994. Energetics of Plant Growth Under Anoxia:
692 Metabolic adaptations of Oryza sativa and Echinochloa phyllopogon. Ann. Bot. 74, 445–
693 455. doi:10.1006/anbo.1994.1140
694 Gálvez, L., González, E.M., Arrese-Igor, C., 2005. Evidence for carbon flux shortage and
695 strong carbon/nitrogen interactions in pea nodules at early stages of water stress. J. Exp.
696 Bot. 56, 2551–2561. doi:10.1093/jxb/eri249
697 Gargallo-Garriga, A., Sardans, J., Pérez-Trujillo, M., Rivas-Ubach, A., Oravec, M., Vecerova,

698 K., Urban, O., Jentsch, A., Kreyling, J., Beierkuhnlein, C., Parella, T., Peñuelas, J., 2014.
699 Opposite metabolic responses of shoots and roots to drought. Sci. Rep. 4, 6829.
700 doi:10.1038/srep06829
701 Geigenberger, P., 2011. Regulation of starch biosynthesis in response to a fluctuating
702 environment. Plant Physiol. 155, 1566–1577. doi:10.1104/pp.110.170399
703 Gewin, V., 2010. Food: An underground revolution. Nature 466, 552–553.
704 doi:10.1038/466552a
705 Gibon, Y., Blaesing, O.E., Hannemann, J., Carillo, P., Höhne, M., Hendriks, J.H.M., Palacios,
706 N., Cross, J., Selbig, J., Stitt, M., 2004. A Robot-based platform to measure multiple
707 enzyme activities in Arabidopsis using a set of cycling assays: comparison of changes of
708 enzyme activities and transcript levels during diurnal cycles and in prolonged darkness.
709 Plant Cell 16, 3304–3325. doi:10.1105/tpc.104.025973
710 Gil-Quintana, E., Larrainzar, E., Arrese-Igor, C., González, E.M., 2013. Is N-feedback
711 involved in the inhibition of nitrogen fixation in drought-stressed Medicago truncatula?
712 J. Exp. Bot. 64, 281–292. doi:10.1093/jxb/ers334
713 Gil, R., Boscaiu, M., Lull, C., Bautista, I., Lidón, A., Vicente, O., 2013. Are soluble
714 carbohydrates ecologically relevant for salt tolerance in halophytes? Funct. Plant Biol.
715 40, 805–818. doi:10.1071/FP12359
716 Gonzalez, E.M., Aparicio-Tejo, P.M., Gordon, A.J., Minchin, F.R., Royuela, M., Arrese-Igor,
717 C., 1998. Water-deficit effects on carbon and nitrogen metabolism of pea nodules. J. Exp.
718 Bot. 49, 1705–1714. doi:10.1093/jxb/49.327.1705
719 González, E.M., Gordon, A.J., James, C.L., Arrese-Igor, C., 1995. The role of sucrose
720 synthase in the response of soybean nodules to drought. J. Exp. Bot. 46, 1515-1523. doi:
721 10.1093/jxb/46.10.1515
722 Graham, P.H., Vance, C.P., 2003. Legumes: importance and constraints to greater use. Plant

723 Physiol. 131, 872–877. doi:10.1104/pp.017004
724 Hatch, M.D., Mau, S.L., 1973. Activity, location, and role of asparate aminotransferase and
725 alanine aminotransferase isoenzymes in leaves with C4 pathway photosynthesis. Arch.
726 Biochem. Biophys. 156, 195–206. doi:10.1016/0003-9861(73)90357-3
727 Hodges, M., Flesch, V., Gálvez, S., Bismuth, E., 2003. Higher plant NADP+-dependent
728 isocitrate dehydrogenases, ammonium assimilation and NADPH production. Plant
729 Physiol. Biochem. 41, 577–585. doi:10.1016/S0981-9428(03)00062-7
730 Hsiao, T.C., 1973. Plant Responses to Water Stress. Annu. Rev. Plant Physiol. 24, 519–570.
731 doi:10.1146/annurev.pp.24.060173.002511
732 Huang, B., Gao, H., 2000. Root physiological characteristics associated with drought
733 resistance in tall fescue cultivars. Crop Sci. 40, 196–203.
734 doi:10.2135/cropsci2000.401196x
735 Kishor, P.B.K., Sangam, S., Amrutha, R.N., Laxmi, P.S., Naidu, K.R., Rao, K.R.S.S., Rao,
736 S.C., Reddy, K.J., Theriappan, P., Sreenivasulu, N., 2005. Regulation of proline
737 biosynthesis, degradation, uptake and transport in higher plants: Its implications in plant
738 growth and abiotic stress tolerance. Curr. Sci. 88, 424–438.
739 Lambers, H., Stulen, I., van der Wert, A., 1996. Carbon use in root respiration as affected by
740 elevated atmospheric O2. Plant Soil 187, 251–263. doi:10.1007/BF00017091
741 Lou, Y., Gou, J.-Y., Xue, H.-W., 2007. PIP5K9, an Arabidopsis Phosphatidylinositol
742 Monophosphate Kinase, Interacts with a Cytosolic Invertase to Negatively Regulate
743 Sugar-Mediated Root Growth. Plant Cell 19, 163–181. doi:10.1105/tpc.106.045658
744 Lynch, J.P., Brown, K.M., 2012. New roots for agriculture: exploiting the root phenome.
745 Philos. Trans. R. Soc. Lond. B. Biol. Sci. 367, 1598–1604. doi:10.1098/rstb.2011.0243
746 Lynch, J.P., Chimungu, J.G., Brown, K.M., 2014. Root anatomical phenes associated with
747 water acquisition from drying soil: targets for crop improvement. J. Exp. Bot. 65, 6155–

748 6166. doi:10.1093/jxb/eru162
749 Marino, D., González, E.M., Arrese-Igor, C., 2006. Drought effects on carbon and nitrogen
750 metabolism of pea nodules can be mimicked by paraquat: evidence for the occurrence of
751 two regulation pathways under oxidative stresses. J. Exp. Bot. 57, 665–673.
752 doi:10.1093/jxb/erj056
753 Miller, G., Stein, H., Honig, A., Kapulnik, Y., Zilberstein, A., 2005. Responsive modes of
754 Medicago sativa proline dehydrogenase genes during salt stress and recovery dictate free
755 proline accumulation. Planta 222, 70–79. doi:10.1007/s00425-005-1518-4
756 Moreau, D (2006) Morphology, development and plant architecture of M. truncatula. In: The
757 Medicago truncatula handbook. Mathesius U, Journet EP, Sumner LW (eds). ISBN 0-
758 9754303-1-9. http://www.noble.org/MedicagoHandbook.
759 Muller, B., Pantin, F., Génard, M., Turc, O., Freixes, S., Piques, M., Gibon, Y., 2011. Water
760 deficits uncouple growth from photosynthesis, increase C content, and modify the
761 relationships between C and growth in sink organs. J. Exp. Bot. 62, 1715–1729.
762 doi:10.1093/jxb/erq438
763 Päpke, C., Ramirez-Aguilar, S., Antonio, C., 2013. Oxygen Consumption Under Hypoxic
764 Conditions, in: Low-Oxygen Stress in Plants. pp. 185–208. doi:10.1007/978-3-7091-
765 1254-0_10
766 Phan, H.T.T., Ellwood, S.R., Hane, J.K., Ford, R., Materne, M., Oliver, R.P., 2007. Extensive
767 macrosynteny between *Medicago truncatula* and *Lens culinaris* ssp. *culinaris*. Theor.
768 Appl. Genet. 114, 549–558. doi: 10.1007/s00122-006-0455-3
769 Phutela, A., Jain, V., Dhawan, K., Nainawatee, H.S., 2000. Proline Metabolism Under Water
770 Stress in the Leaves and Roots of Brassica juncea Cultivars Differing in Drought
771 Tolerance. J. Plant Biochem. Biotechnol. 9, 35–39. doi:10.1007/BF03263081
772 Pires, M. V., Pereira Junior, A.A., Medeiros, D.B., Daloso, D.M., Pham, P.A., Barros, K.A.,

773 Engqvist, M.K.M., Florian, A., Krahnert, I., Maurino, V.G., Araújo, W.L., Fernie, A.R.,
774 2016. The influence of alternative pathways of respiration that utilize branched-chain
775 amino acids following water shortage in Arabidopsis. Plant Cell Environ. 39, 1304–
776 1319. doi:10.1111/pce.12682
777 Ramos, M.L.G., Gordon, A.J., Minchin, F.R., Sprent, J.I., Parsons, R., 1999. Effect of water
778 stress on nodule physiology and biochemistry of a drought tolerant cultivar of common
779 bean (*Phaseolus vulgaris* L.). *Ann. Bot.* 83, 57-63.
780 Rouached, A., Slama, I., Zorrig, W., Jdey, A., Cukier, C., Rabhi, M., Talbi, O., Limami, A.M.,
781 Abdelly, C., Limami, M.A., Abdelly, C., 2013. Differential performance of two forage
782 species, Medicago truncatula and Sulla carnosa, under water-deficit stress and recovery.
783 Crop Pasture Sci. 64, 254–264. doi:10.1071/CP13049
784 Ruan, Y.-L., Jin, Y., Yang, Y.-J., Li, G.-J., Boyer, J.S., 2010. Sugar Input, Metabolism, and
785 Signaling Mediated by Invertase: Roles in Development, Yield Potential, and Response
786 to Drought and Heat. Mol. Plant 3, 942–955. doi:10.1093/mp/ssq044
787 Ryšlavá, H., Müller, K., Semorádová, Š., Synková, H., Čeřovská, N., 2003. Photosynthesis
788 and activity of phosphoenolpyruvate carboxylase in Nicotiana tabacum L. leaves infected
789 by Potato virus A and Potato virus Y. Photosynthetica 41, 357–363.
790 doi:10.1023/B:PHOT.0000015459.22769.bf
791 Scholander, P.F., Bradstreet, E.D., Hemmingsen, E.A., Hammel, H.T., 1965. Sap Pressure in
792 Vascular Plants: Negative hydrostatic pressure can be measured in plants. Science (80-.).
793 148, 339–346. doi:10.1126/science.148.3668.339
794 Shen, W., Wei, Y., Dauk, M., Tan, Y., Taylor, D.C., Selvaraj, G., Zou, J., 2006. Involvement of
795 a glycerol-3-phosphate dehydrogenase in modulating the NADH/NAD+ ratio provides
796 evidence of a mitochondrial glycerol-3-phosphate shuttle in Arabidopsis. Plant Cell 18,
797 422–441. doi:10.1105/tpc.105.039750

798 Staswick, P.E., 1994. Storage Proteins of Vegetative Plant Tissues. Annu. Rev. Plant Physiol.
799 Plant Mol. Biol. 45, 303–322. doi:10.1146/annurev.pp.45.060194.001511
800 Stitt, M., 1998. Pyrophosphate as an energy donor in the cytosol of plant cells: an enigmatic
801 alternative to ATP. Bot. Acta 111, 167–175. doi:10.1111/j.1438-8677.1998.tb00692.x
802 Sutka, M.R., Manzur, M.E., Vitali, V.A., Micheletto, S., Amodeo, G., 2016. Evidence for the
803 involvement of hydraulic root or shoot adjustments as mechanisms underlying water
804 deficit tolerance in two Sorghum bicolor genotypes. J. Plant Physiol. 192, 13–20.
805 doi:10.1016/j.jplph.2016.01.002
806 Szabados, L., Savouré, A., 2010. Proline: a multifunctional amino acid. Trends Plant Sci. 15,
807 89–97. doi:10.1016/j.tplants.2009.11.009
808 Takizawa, K., Nakamura, H., 1998. Separation and Determination of Fluorescein
809 Isothiocyanate-Labeled Amino Acids by Capillary Electrophoresis with Laser-Induced
810 Fluorescence Detection. Anal. Sci. 14, 925–928. doi:10.2116/analsci.14.925
811 Tian, H., De Smet, I., Ding, Z., 2014. Shaping a root system: regulating lateral versus primary
812 root growth. Trends Plant Sci. 19, 426–431. doi:10.1016/j.tplants.2014.01.007
813 Vargas, W.A., Salerno, G.L., 2010. The Cinderella story of sucrose hydrolysis:
814 Alkaline/neutral invertases, from cyanobacteria to unforeseen roles in plant cytosol and
815 organelles. Plant Sci. 178, 1–8. doi:10.1016/j.plantsci.2009.09.015
816 Verdoy, D., Coba de la Pena, T., Redondo, F.J., Lucas, M.M., Pueyo, J.J., 2006. Transgenic
817 Medicago truncatula plants that accumulate proline display nitrogen-fixing activity with
818 enhanced tolerance to osmotic stress. Plant, Cell Environmen 29, 1913–1923.
819 doi:10.1111/j.1365-3040.2006.01567.x
820 Virlouvet, L., Jacquemot, M.-P., Gerentes, D., Corti, H., Bouton, S., Gilard, F., Valot, B.,
821 Trouverie, J., Tcherkez, G., Falque, M., Damerval, C., Rogowsky, P., Perez, P., Noctor,
822 G., Zivy, M., Coursol, S., 2011. The ZmASR1 protein influences branched-chain amino

823 acid biosynthesis and maintains kernel yield in maize under water-limited conditions.
824 Plant Physiol. 157, 917–936. doi:10.1104/pp.111.176818
825 Waisel, Y., Radunz, A., 2006. Differences in lipid and in fatty acid composition of taproots
826 and lateral roots of faba bean plants (Vicia faba L.) grown in saline media. Plant Biosyst.
827 140, 94–99. doi:10.1080/11263500500520349
828 Winter, H., Huber, S.C., 2000. Regulation of Sucrose Metabolism in Higher Plants:
829 Localization and regulation of Activity of Key Enzymes. Crit. Rev. Biochem. Mol. Biol.
830 19, 31–67. doi:10.1080/07352680091139178
831 Wood, T., 1968. The inhibition of pyruvate kinase by ATP. Biochem. Biophys. Res. Commun.
832 31, 779–785. doi:10.1016/0006-291X(68)90630-X
833 Woodfield, D.R., Caradus, J.R., Cousins, G.R., Dunn, T., 1996. Response to selection for
834 increased taproot diameter. Agron. Soc. New Zeal. 11, 141–144.
835 Zahran, H.H., 1999. Rhizobium-legume symbiosis and nitrogen fixation under severe
836 conditions and in an arid climate. Microbiol. Mol. Biol. Rev. 63, 968–989.
837 Zhan, A., Schneider, H., Lynch, J.P., 2015. Reduced Lateral Root Branching Density
838 Improves Drought Tolerance in Maize. Plant Physiol. 168, 1603–1615.
839 doi:10.1104/pp.15.00187
840 Zrenner, R., Salanoubat, M., Willmitzer, L., Sonnewald, U., 1995. Evidence of the crucial role
841 of sucrose synthase for sink strength using transgenic potato plants (Solanum tuberosum
842 L.). Plant J. 7, 97–107. doi:10.1046/j.1365-313X.1995.07010097.x
843
844

Figure 1

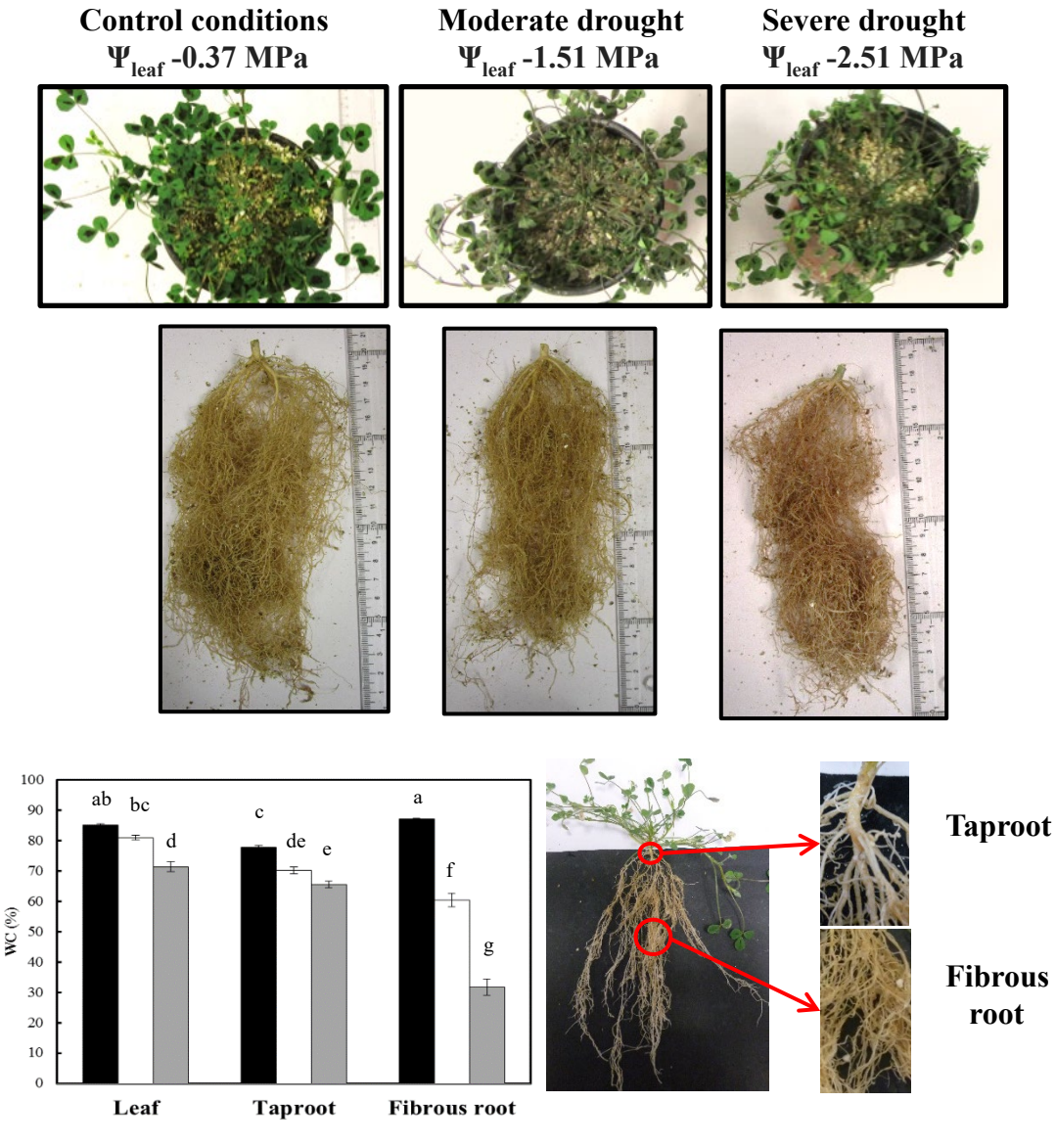
Control conditions
Ψ_{leaf} -0.37 MPa
Moderate drought
Ψ_{leaf} -1.51 MPa
Severe drought
Ψ_{leaf} -2.51 MPa
WC (%)
100
90
80
70
60
50
40
30
20
10
0
ab
bc
d
c
de
e
a
f
g
Leaf
Taproot
Fibrous root
Taproot
Fibrous root

Figure 2

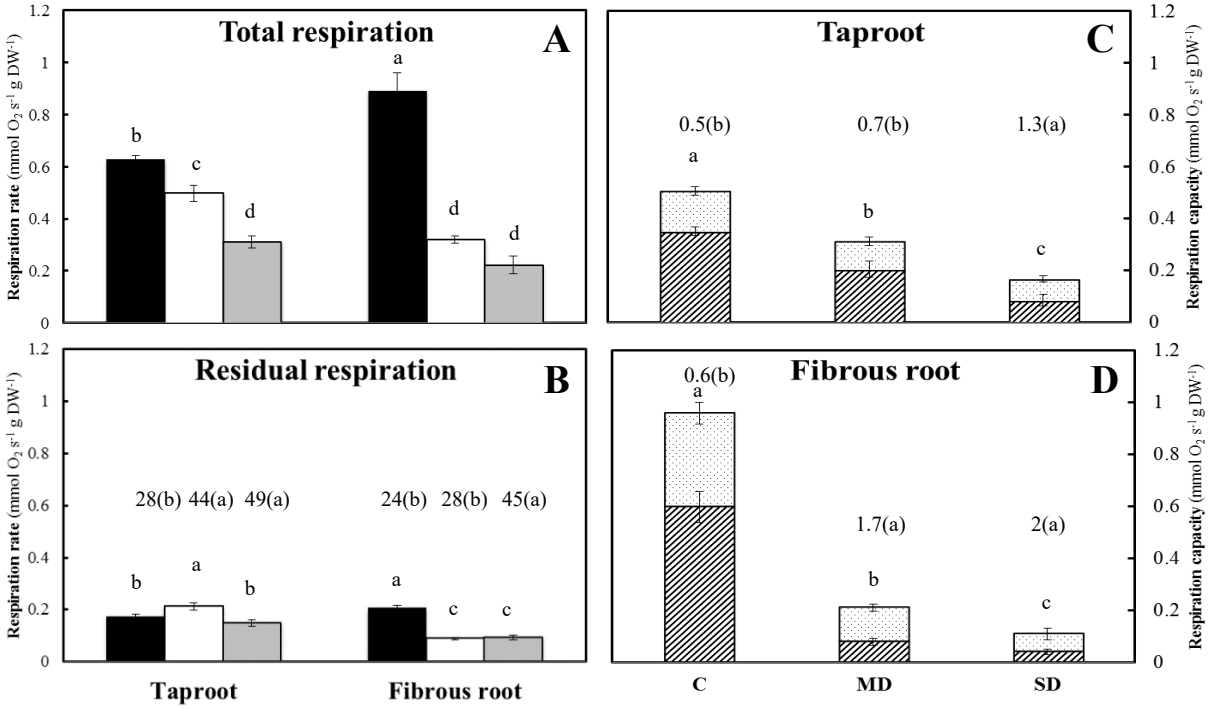
Total respiration
A
Taproot
C
Residual respiration
B
Fibrous root
D
Respiration rate (nmol O2 s-1 g DW-1)
Respiration capacity (nmol O2 s-1 g DW-1)
0.5(b)
0.7(b)
1.3(a)
28(b) 44(a) 49(a)
24(b) 28(b) 45(a)
0.6(b)
1.7(a)
2(a)
Taproot
Fibrous root
C
MD
SD

Figure 3

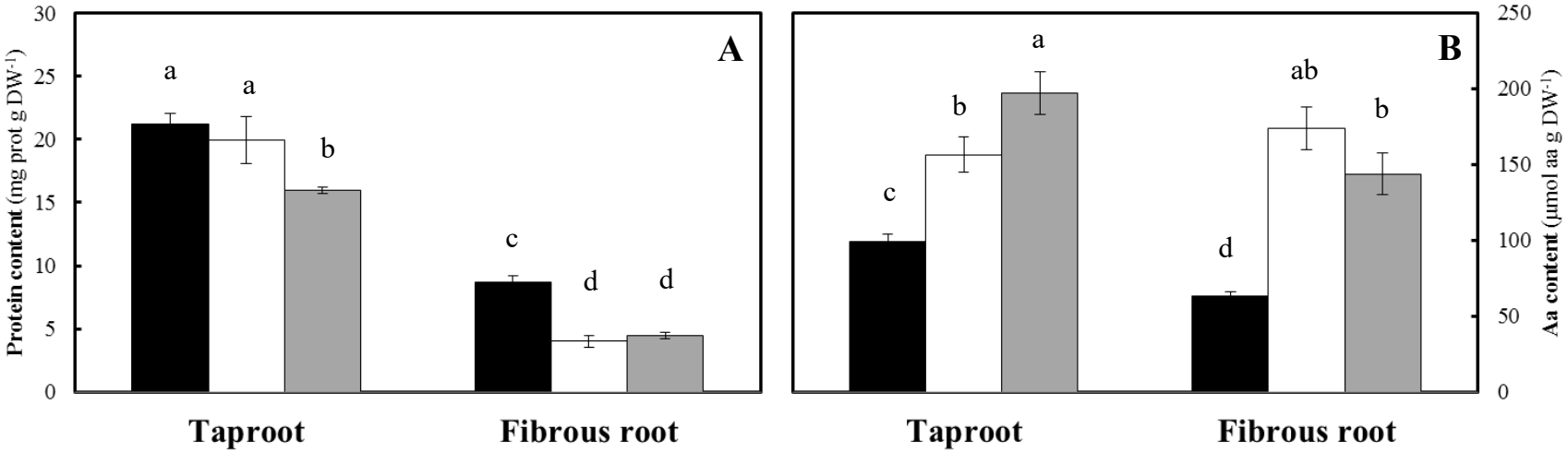
A
B
Protein content (mg prot g DW-1)
Aa content (µmol aa g DW-1)
30
25
20
15
10
5
0
250
200
150
100
50
0
a
a
b
c
d
d
c
b
a
d
ab
b
Taproot
Fibrous root
Taproot
Fibrous root

Figure 4

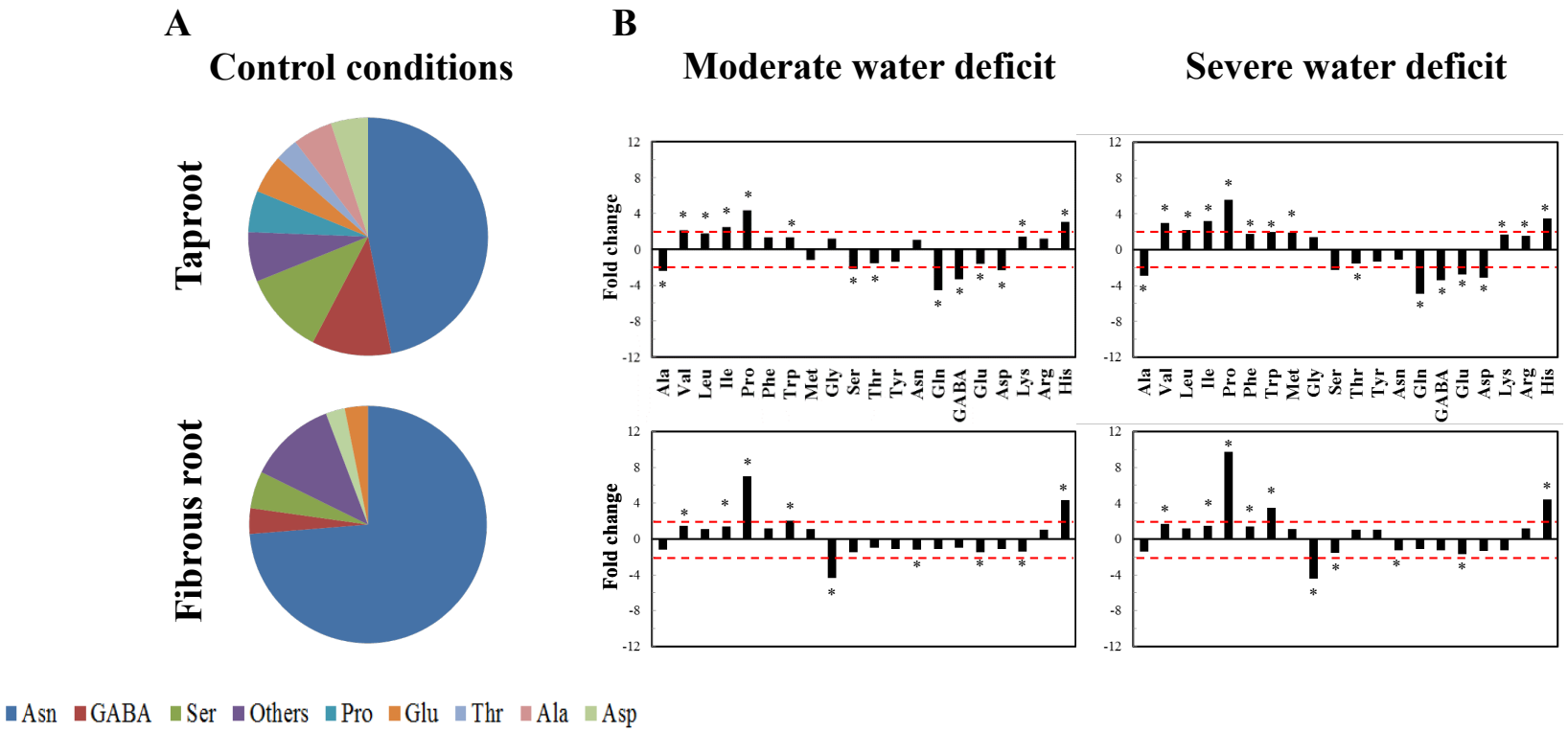
A
Control conditions
Taproot
Fibrous root
B
Moderate water deficit
Severe water deficit
Fold change
12
8
4
0
-4
-8
-12
Ala Val Leu Ile Pro Phe Trp Met Gly Ser Thr Tyr Asn Gln GABA Glu Asp Lys Arg His
Asn GABA Ser Others Pro Glu Thr Ala Asp

Figure 5

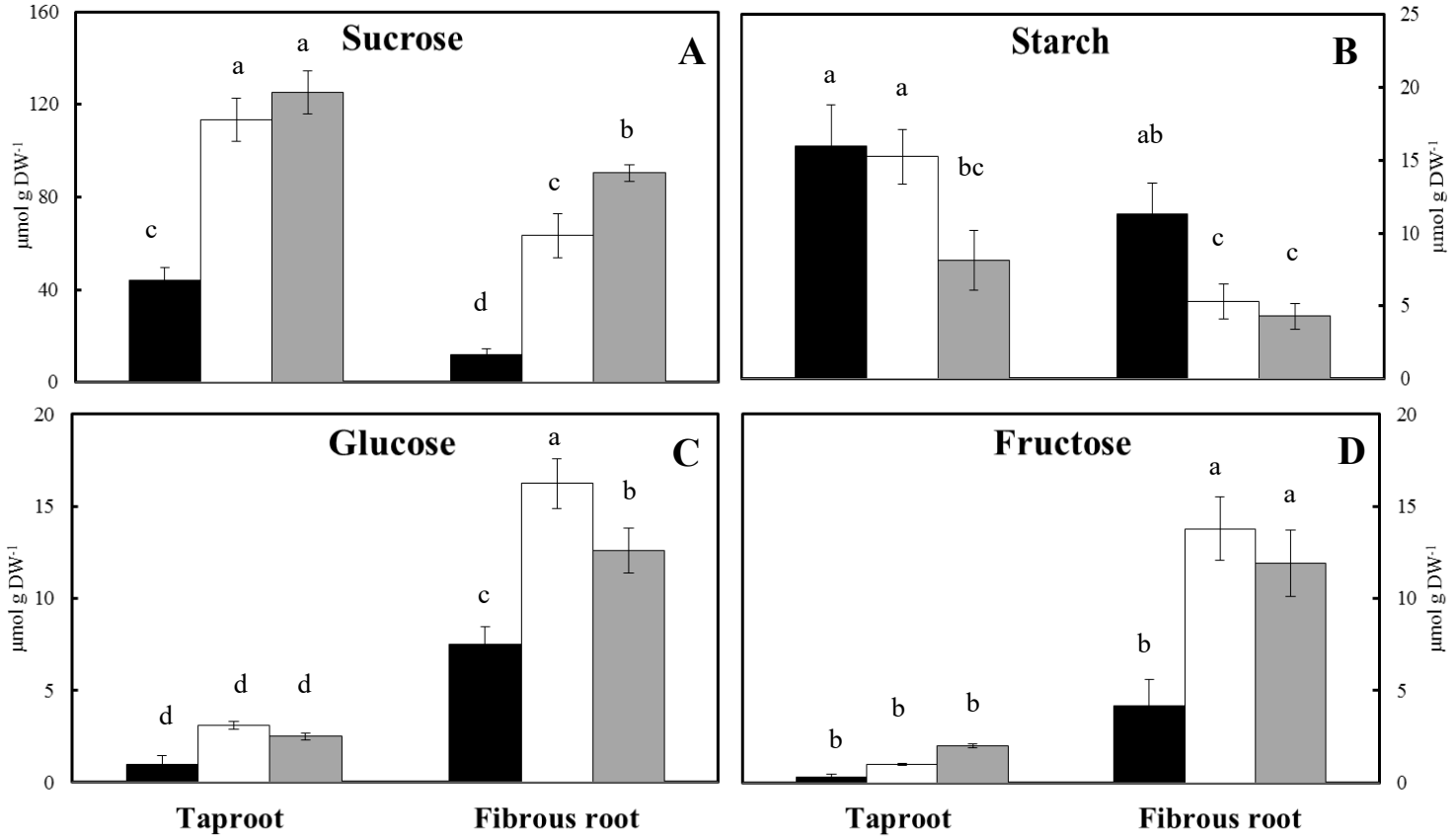
Sucrose
A
Starch
B
Glucose
C
Fructose
D
µmol g DW-1
Taproot
Fibrous root
160
120
80
40
0
25
20
15
10
5
c
a
a
d
c
b
a
a
bc
ab
c
c
d
d
d
a
c
b
b
b
b
b
a
a

Figure 6

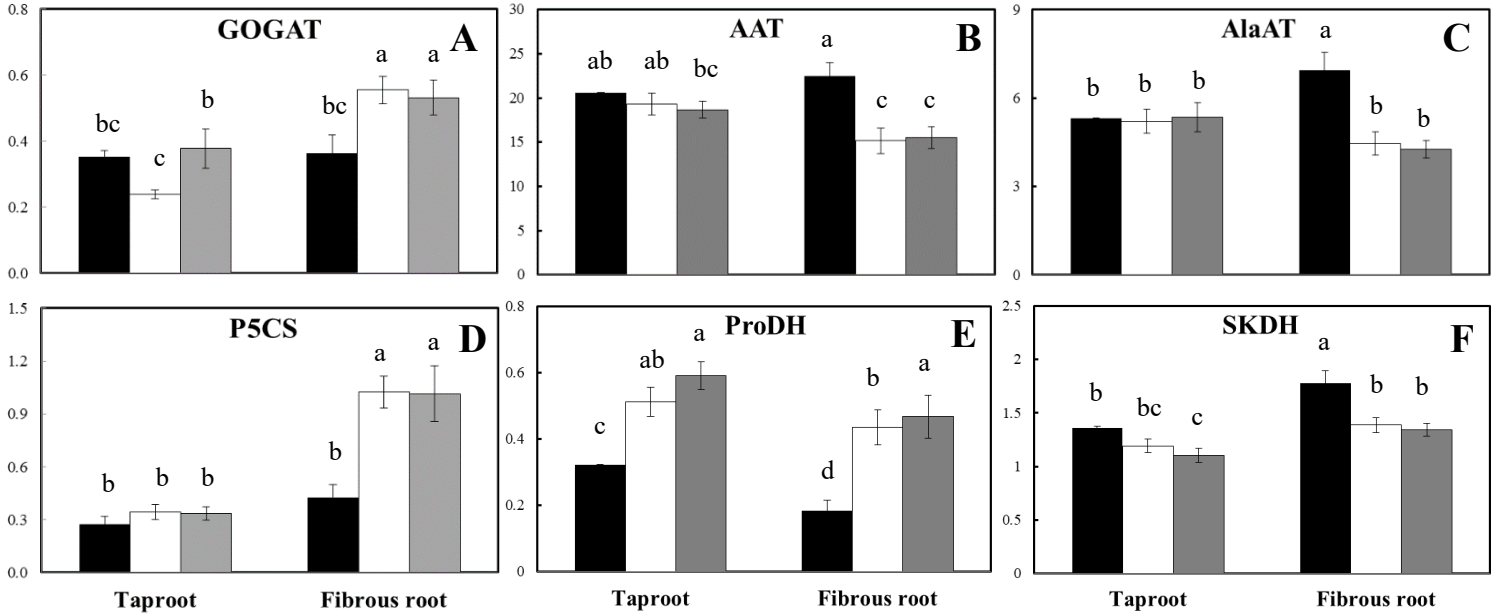
GOGAT
A
bc
c
b
bc
a
a
AAT
B
ab
ab
bc
a
c
c
AlaAT
C
b
b
b
a
b
b
P5CS
D
b
b
b
b
a
a
ProDH
E
c
ab
a
d
b
a
SKDH
F
b
bc
c
a
b
b
Taproot
Fibrous root
Taproot
Fibrous root
Taproot
Fibrous root

Figure 7

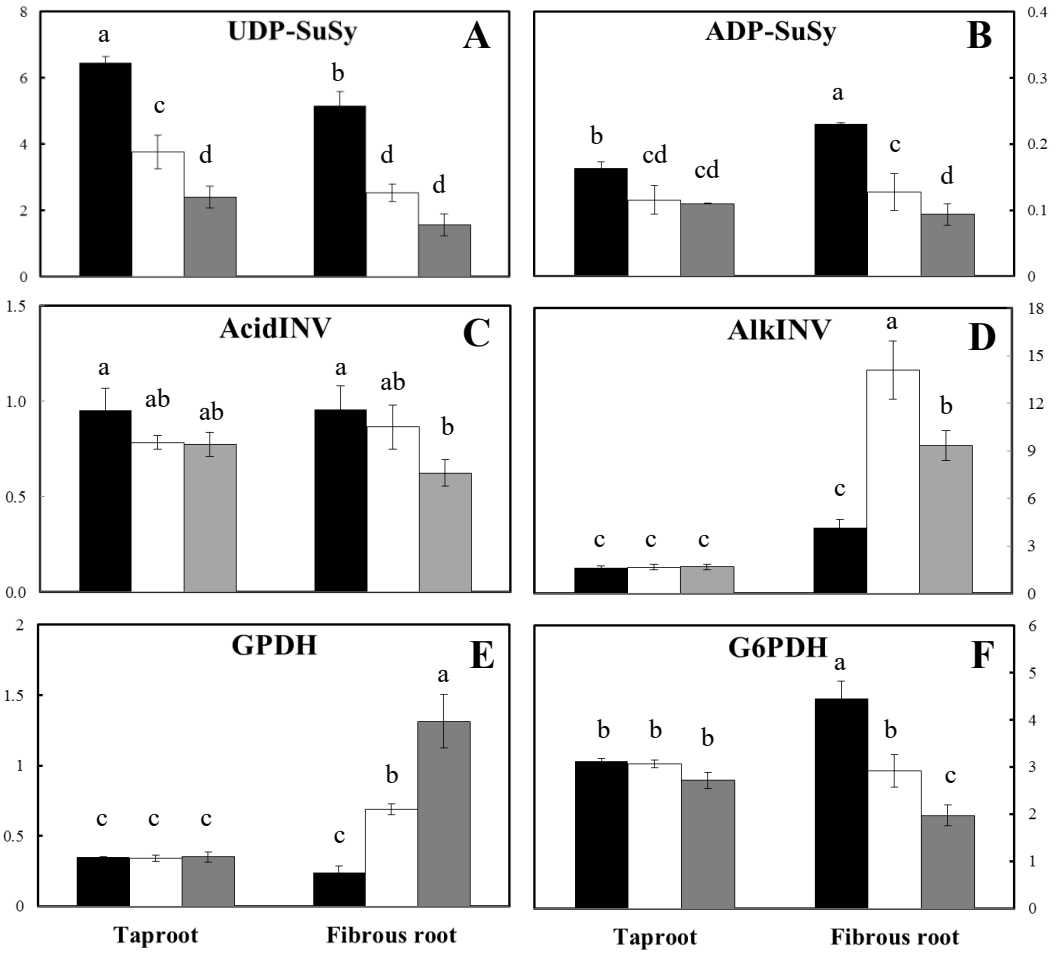
UDP-SuSy
A
ADP-SuSy
B
AcidINV
C
AlkINV
D
GPDH
E
G6PDH
F
Taproot
Fibrous root
Taproot
Fibrous root

Figure 8

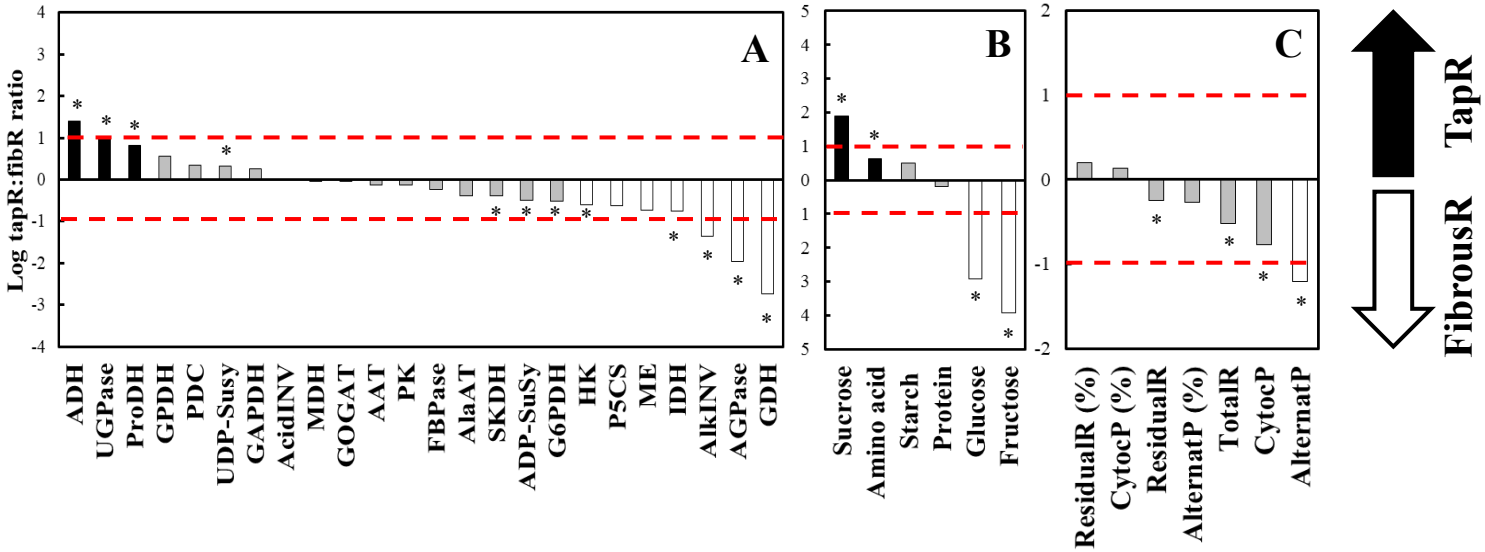
Log tapR:fibR ratio
A
B
C
ADH
UGPase
ProDH
GPDH
PDC
UDP-Susy
GAPDH
AcidINV
MDH
GOGAT
AAT
PK
FBPase
AlaAT
SKDH
ADP-SuSy
G6PDH
HK
P5CS
ME
IDH
AlkINV
AGPase
GDH
Sucrose
Amino acid
Starch
Protein
Glucose
Fructose
ResidualR (%)
CytocP (%)
ResidualR
AlternatP (%)
TotalR
CytocP
AlternatP
TapR
FibrousR

Figure S1

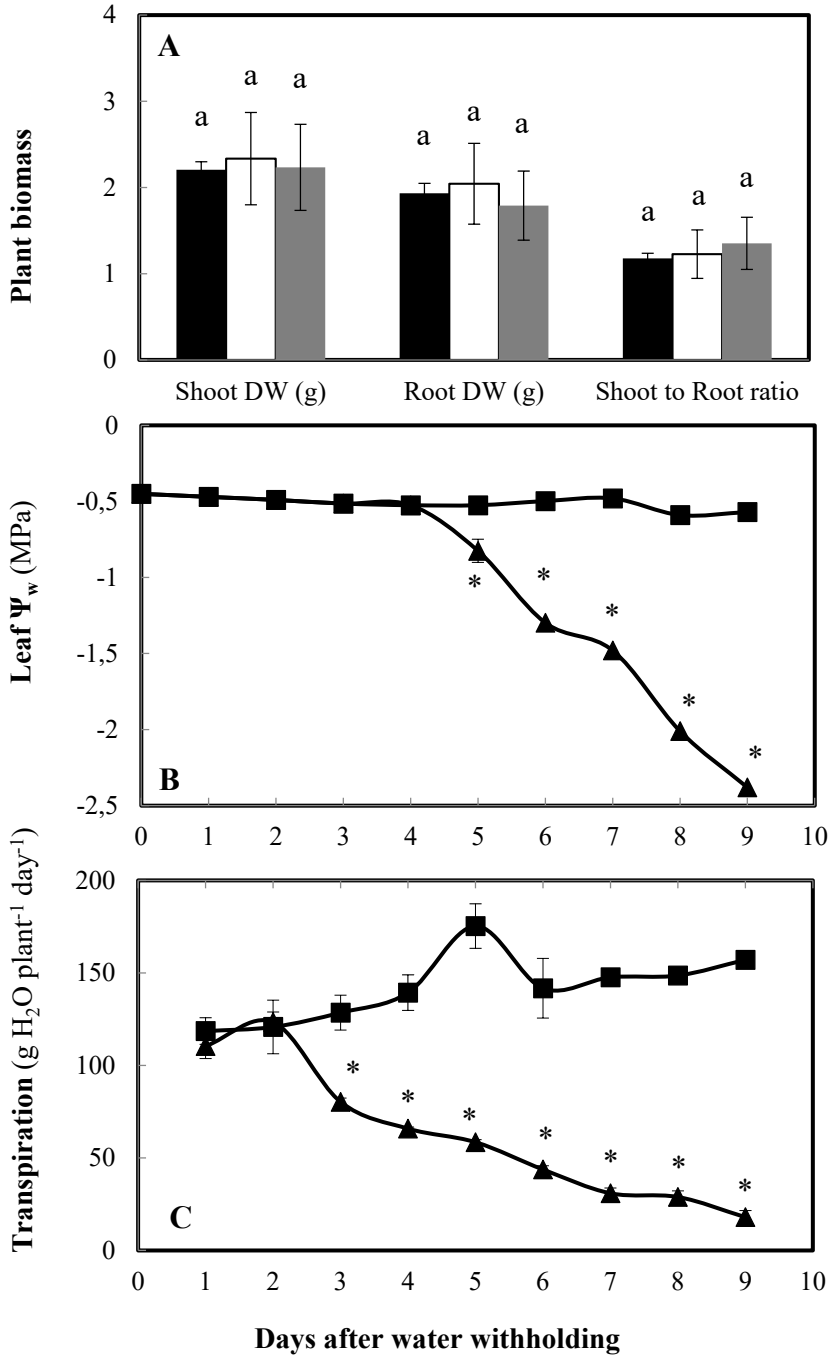
A
Plant biomass
Shoot DW (g)
Root DW (g)
Shoot to Root ratio
B
Leaf Ψ_w (MPa)
C
Transpiration (g H_2O plant^{-1} day^{-1})
Days after water withholding

Figure S2

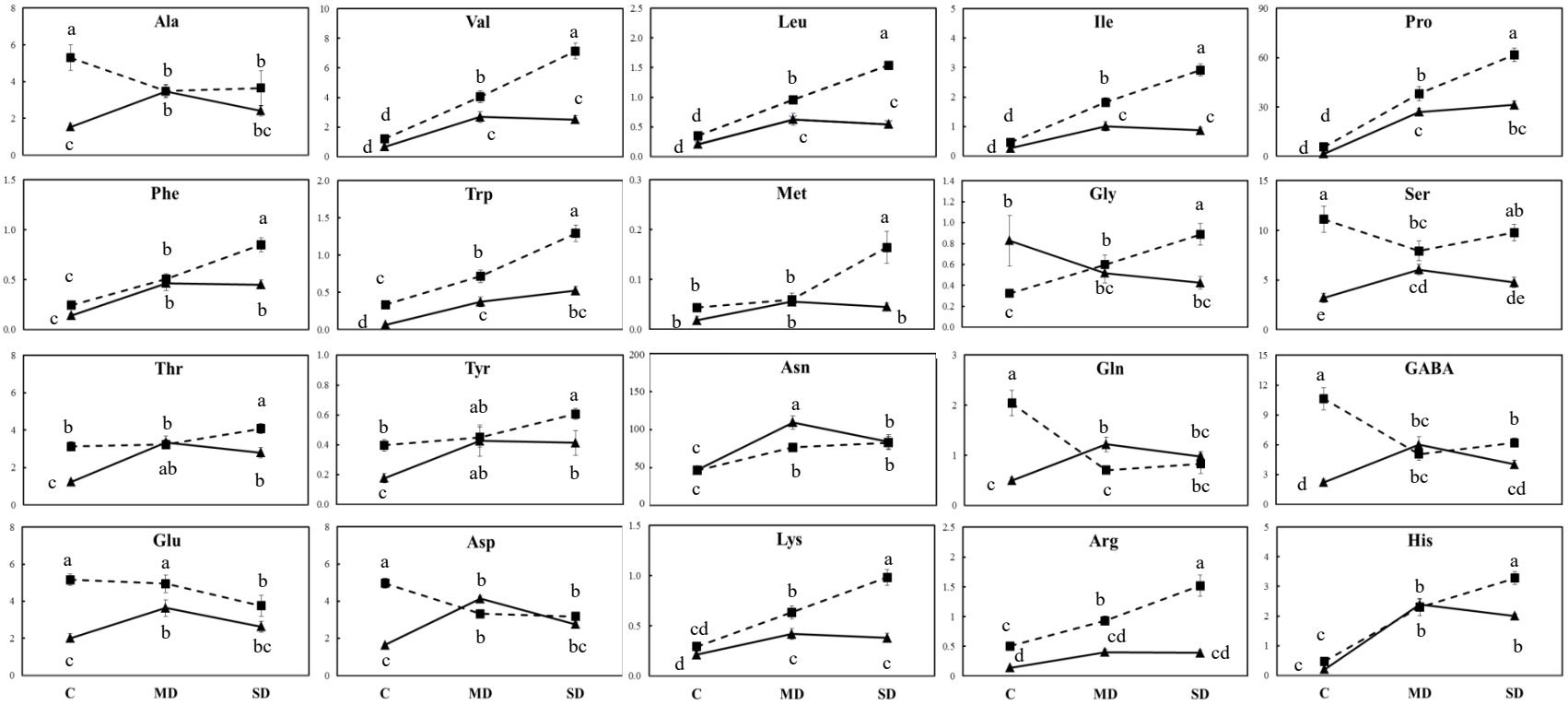
Ala
Val
Leu
Ile
Pro
Phe
Trp
Met
Gly
Ser
Thr
Tyr
Asn
Gln
GABA
Glu
Asp
Lys
Arg
His
C
MD
SD

Figure S3

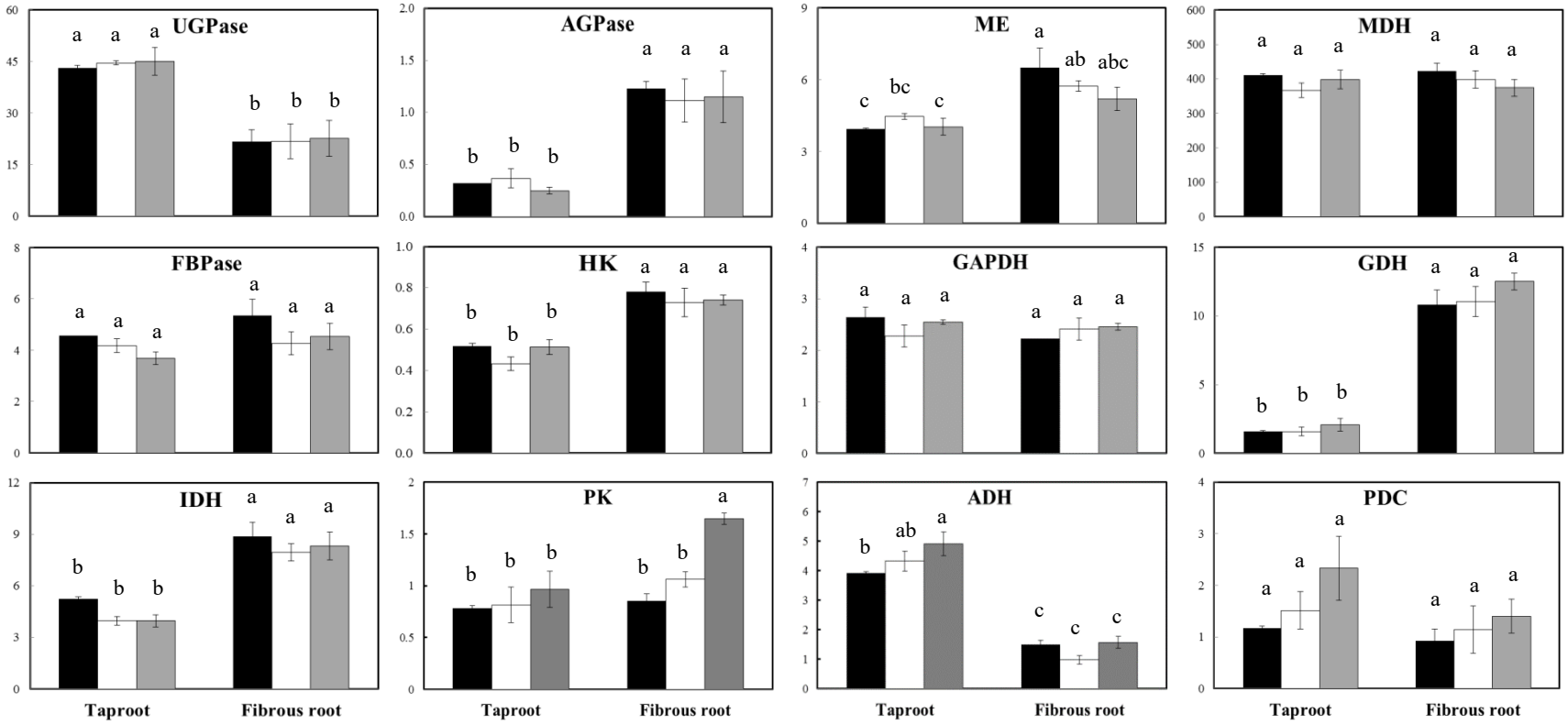
UGPase
AGPase
ME
MDH
FBPase
HK
GAPDH
GDH
IDH
PK
ADH
PDC
Taproot
Fibrous root

Table S1

Root type	Treatment	Total respiration	Residual respiration	Alternative pathway capacity	Cytochrome pathway capacity
Taproot	C	0.63 ± 0.01 [b]	0.17 ± 0.01 [b]	0.16 ± 0.02 [b]	0.35 ± 0.02 [b]
	MD	0.50 ± 0.03 [c]	0.21 ± 0.01 [a]	0.11 ± 0.02 [bc]	0.20 ± 0.03 [c]
	SD	0.31 ± 0.02 [d]	0.15 ± 0.01 [b]	0.08 ± 0.01 [c]	0.08 ± 0.02 [d]
Fibrous root	C	0.89 ± 0.07 [a]	0.20 ± 0.01 [a]	0.36 ± 0.04 [a]	0.60 ± 0.06 [a]
	MD	0.32 ± 0.01 [d]	0.09 ± 0.01 [c]	0.13 ± 0.01 [bc]	0.08 ± 0.01 [d]
	SD	0.22 ± 0.03 [d]	0.09 ± 0.01 [c]	0.07 ± 0.02 [c]	0.04 ± 0.01 [d]

Table S2

A

WC & Respiration	WD	Organ	WD * Organ
Water content	***	***	***
Shoot DW	ns	ns	ns
Root DW	ns	ns	ns
Shoot to Root ratio	ns	ns	ns
Total respiration	***	ns	***
Residual respiration	***	***	***
Residual respiration (%)	***	**	ns
Cytochromic capacity	***	ns	***
Alternative capacity	***	***	***
Cyt + Aox capacities	***	*	***
Aox : Cyt capacity ratio	**	*	ns

B

C compounds	WD	Organ	WD * Organ
Starch	**	***	ns
Sucrose	***	***	ns
Glucose	***	***	**
Fructose	***	***	**

C

C metabolism	WD	Organ	WD * Organ
UDP-SuSy	***	**	ns
ADP-SuSy	***	*	**
AcidINV	**	ns	ns
AlkINV	***	***	***
GPDH	***	***	***
G6PDH	***	ns	**

D

N compounds	WD	Organ	WD * Organ
Soluble protein	***	***	ns
Total amino acid	***	*	*
Ala	***	***	***
Val	***	***	***
Leu	***	***	***
Ile	***	***	***
Pro	***	***	*
Phe	**	***	ns
Trp	***	***	ns
Met	**	ns	ns
Gly	ns	**	***
Ser	***	***	***
Thr	***	***	***
Tyr	ns	ns	ns
Asn	***	***	**
Gln	**	***	***
GABA	***	***	***
Glu	***	***	**
Asp	*	***	**
Lys	***	*	***
Arg	***	**	ns
His	ns	***	ns

E

N metabolism	WD	Organ	WD * Organ
GOGAT	ns	***	**
AAT	**	ns	*
AlaAT	**	ns	**
P5CS	***	***	**
ProDH	***	**	ns
SKDH	***	**	ns